Main authors response:

The referees clearly highlight that major challenges in debris flow model research are the accurate treatment of the phase interactions between the granular and fluid components, and taking physical processes related to granular flow into account. We agree. In response to the Referees' comments, we point out that in our model the fluid-grain and grain-grain interactions of larger particles are introduced with a coupled Lagrangian particle approach. The Referees mainly objected to our relatively simple treatment of the coupling, where we neglect inter-phase momentum exchange. To help justify our plans to present the solver as it is now, we include additional Figures in this response letter (not intended to be included in the final manuscript). The two main points that we would like to illustrate is that there are advantages arising from the 3-dimensional approach, even without inter-phase momentum exchange, and that the inter-phase momentum exchange is of relatively minor importance in the applications described in this manuscript, which in turn is due to the large concentration of fine material.

The main point that we would like to make in this manuscript is that we can model, in 3D, many practical aspects of the flow of muddy debris flows with only one free parameter (Figure 1, in this letter–please note that this Figure is an application of a previous version of this model and is not appropriate for inclusion within this manuscript). If we were to include the extensions proposed by the Referees, we must then introduce more coefficients that must be fitted (instead of independently measurable quantities) which would in turn introduce additional uncertainties in the application to real-world engineering problems. Because the basic method itself follows a new strategy by solving the transport equations in 3D and by limiting the number of free model parameters, we think that the basic method is already of interest and should be presented and published before including the extensions. As it stands, the model is already of use to practitioners due to the small number of adjustable coefficients which can be defined based on measurable material properties.

We are already working on the development of an additional diffusive term (drift-flux approach) in the advection-dispersion equation of the gravel phase that depends on the local Savage number, to permit modelling of the phase separation in the grain-inertia flow regime (abstract submitted to the 2016 EGU meeting). However, this approach also includes a coupled Langrangian particle simulation. In our opinion, these new extensions would overwhelm the present manuscript and dilute our main point with the introduction of additional parameters. We mention that these extensions are in development, however, to help the reader to see the longer-term trajectory of this modeling effort.

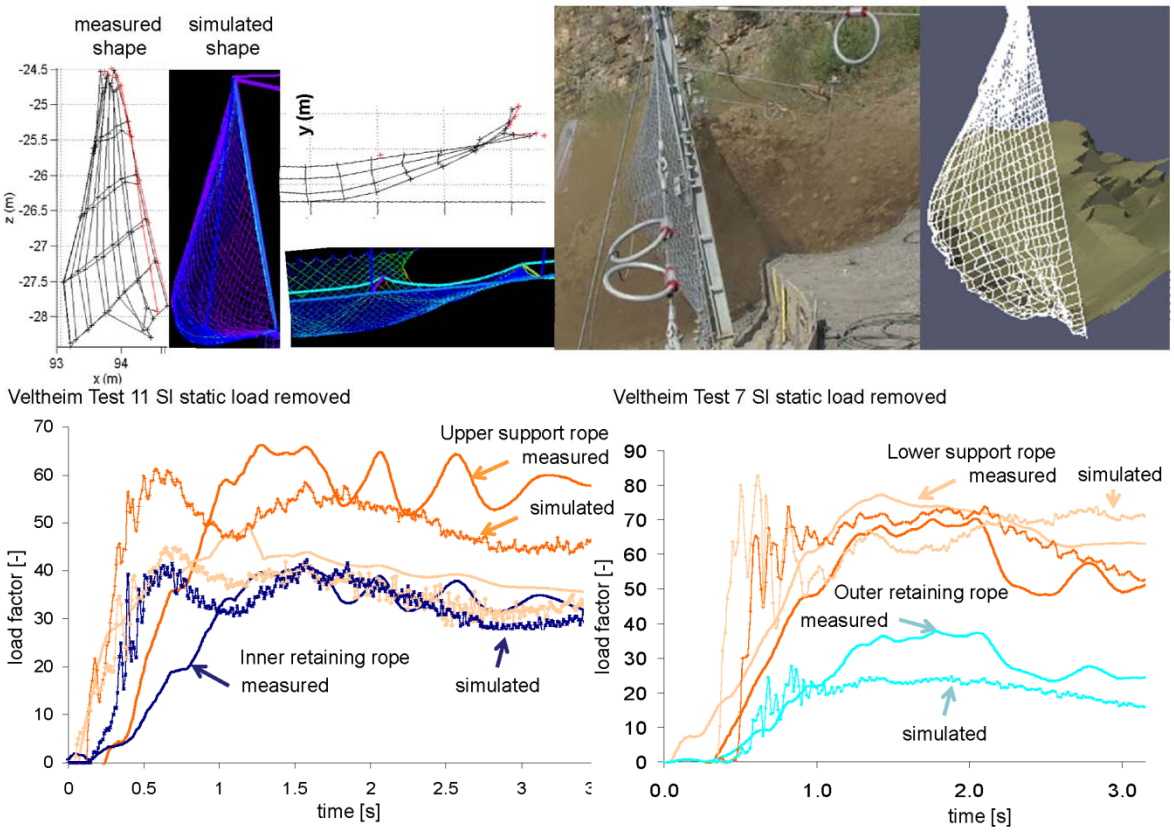

Fig. 1: Debris flow impact into a flexible barriers, experiments and corresponding simulations performed with the CFD solver interDyMFoam coupled to the DEM code FARO. Upper left: measured and simulated final barrier deformation, upper right: side-view of the barrier under maximal load and corresponding CFD material body with FSI interface (white). Bottom: comparison of simulated and modeled rope forces (scaled to maximal load = 100) within the barrier structure for two different barrier types and material mixtures. A Herschel-Bulkley rheology model was used.

Authors' responses to issues raized by Referee #1 and Referee #2

Referee #1 *stated that the rheological models and the basis of the CFD software already exist and that the manuscript did not present substantial advancement in modelling debris flows. According to* ***referee #1*** *the main deficiency lies in the Volume Of Fluid approach without momentum exchange between the granular and the fluid phase and that one thereby neglects parts of the physics of the two phase flow problem. It is stated that the passive and very weak connection between the phases via cell-averaged bulk kinematic viscosity isn't a sufficient interaction between phases and that drag etc. must be included in momentum and transport equations to be justified physically.*

Yes, we agree that we use existing CFD software (as well as existing concepts) to make our main point in the manuscript. However, this paper combines them in a unique and useful manner. All currently applied debris flow models that use a two-phase description of the debris-flow material are depth-averaged or 2D. Three dimensional debris-flow models with momentum exchange between phases have, up to now, been limited to academic cases, because their

numerical costs are about ten times higher than the Volume of Fluid (VOF) approach. The currently available models also contain many parameters that must be fitted to site-specific field data, severely limiting their applicability to real-world problems and also their usefulness for scientific hypothesis testing.

Our approach seeks to overcome some of these limitations. Our model has to be seen as a first step and it is already at the limit of feasibility due to high computational costs. We aim to gain experience from the applied community's use of the Volume of Fluid approach, which allows us to face real-world problems. The main new points in this paper are the new ability to move beyond the depth-averaged perspective, to account for the three-dimensional flow structure and its interaction with a pressure-dependent rheology model, and to reduce the number of free parameters. The phase effects presented here arise from pressure- and shear-rate-sensitive viscosity that depends on the local phase concentrations. Our assumptions are valid for viscous debris flows with high contents of clay, silt and sand that damp the granular collisions between gravel particles, so our model is indeed limited to a specified range of debris flows. As described above, the manuscript is an introduction into the new model concept. Therefore the introduction of dynamically changing phase concentrations distracts from the main idea. In the revised manuscript, we now introduce the solver concept in the beginning to make this clear. We now highlight the first-stage level of the model with its focus on phase-dependent rheology and the possibilities to introduce inter-phase momentum exchange with future extensions:

"Multiphase flows of gas, fluid and sediment can be addressed with the so-called mixture- or driftflux model in cases where the local difference in phase velocities is small (Bohorquez, 2008). The properties of all phases are cell-averaged to derive a single mass continuity and momentum balance equation describing the entire mixture. The model presented here has to be seen as a first step, assuming that the local velocity of the gravel is about the same as the velocity of the surrounding fluid, thus allowing us to neglect the drift-flux. This assumption would not be valid for debris flows with little interstitial fluid, or with interstitial fluid of small viscosity (i. e., a slurry with low concentrations of fine material). The assumption of equal velocities of both phases in one cell leads to a constant composition of the mixture by means of phase concentrations over the entire flow process. This basic model can be seen as a counterpart to the mixture model of Iverson and Denlinger (2001), extended by resolving the three dimensional flow structure in combination with a pressure and shear-rate-dependent rheology linked to the material composition. In future work, we aim to relax the constraint of equal phase velocities and allow dispersion of constituents by introducing relative velocities of the gravel phase with respect to the fine sediment suspension according to Bohorquez (2012) and Damián (2013) together with a coupled Lagrangian particle simulation that can account for larger grains. The basic model presented here focuses on the role of pressure-dependent flow behavior of the gravel, in combination with the shear-dependent rheology of the slurry."

Referee #1 *questioned the model name DebrisInterMixing-2.3*

The model is a direct derivative of the OpenFOAM solver branch "interMixing" extended for debris flows. The Numbers in the title indicate the corresponding version number of the OpenFOAM release.

Referee 1 *points out a discrepancy in our statements, where we mention the change in phase compositions as one source for the limited applicability of previous models, while our model cannot handle dynamic change in granular and viscous concentrations during the flow process itself.*

We applied the model to debris flows with high concentrations of fine particle suspensions that were released in a homogeneous mixture with gravel. In this range of application, the dynamic change in concentrations has a minor effect on the flow process, compared to the influence of the pressure and shear rate dependency of the rheology. Our advance in modeling debris flows is from accounting for the role of the pressure as part of the energy dissipation in dependency to the gravel content which allows us to introduce a material-composition-dependent influence of the three-dimensional pressure field on the flow. We revised the manuscript accordingly to more clearly focus on the main points of pressure dependency and automated adaptation of the rheology to changed material compositions. However, since we see the importance of changing phase compositions in case of debris flows that are dominated by granular flow processes, we mention the change in phase compositions as one factor that limits the applicability of debris-flow models. We use this statement to explain why we implemented the advection-diffusion equation for each mixing phase separately. We explain the strategy accordingly:

"However, to allow evolving phase concentrations between the mixing phases of the slurry and the gravel in future releases, our modified version of the interMixingFoam solver applies eq. 6 separately to each mixing phase including diffusion:"

Referee #1 *states that as the density and viscosity of the air are negligible as compared to those values of interstitial fluid in the debris mixture, considering ambient air (calling it a third phase), which has no extra mechanical consequence in the flow dynamics, is of little, or no use.*

The gas phase has mechanical consequence through the free surface formation that may lead to large air inclusions in case of impacts or flows over steps, as can be seen in the standard case included in Fig. 5. We now clearly position our model as an extension of the mixture model of Iverson & Dendlinger (2001) but with the capability to be extended to a multiphase flow model with inter-phase momentum exchange and phase concentrations as a dynamic field variable. However, here we focus on the capability of modeling debris flows in complex geometries with a single free model parameter.

Referee #1 *says that we should try to understand the real and important physics of flow, deformation and interactions between phases rather than neglecting or avoiding it, that the recent debris flow modelling trend is trying to address these challenges. It is stated that substantial recent research works on two-phase debris flows with non-zero relative velocity between phases and other higher order interacting terms and advanced physics of flow were not addressed in the manuscript.*

This comment made us aware that the main point of our paper was not explained sufficiently. As described elsewhere, we have strengthened the focus on application. We are not aware of the work Referee 1 refers to here (no citations were provided), however we would certainly be happy to include relevant references to such work, especially if they are applicable to solving real-world problems. Our approach is not primarily aimed at advancing the state of the art in theoretical models used in research, but rather at improving the models that are applied to real-world problem-solving, and our literature review was oriented toward the latter rather than the former. We have tried to make this clearer in the revision.

Referee #1 *raises several concerns about how the governing equations and boundary conditions are applied to the granular phase.*

The original manuscript did not cover the equations as applied in the model, instead we presented a brief introduction into the Finite Volume approach. We have now rewritten the manuscript accordingly to show the applied concept of the Volume Of Fluid implementation in detail.

Referee #2 *states that the main weakness of the paper is that the authors promise a two (or three?) phase debris flow model (abstract, introduction), but it turns out that effectively it is a one-phase flow model without substantial new insights of the real physics of deforming sediment fluid mixtures. An "equivalent fluid" approach might better describe the model.*

The VOF approach is a numerical method for multiphase flow simulations. The VOF method is a surface-tracking technique that allows calculating the volume fraction of each fluid by solving one single momentum equation. However, the core of the method is to efficiently model immiscible multiphase flows, and it is used here to distinguish between the air phase and the bulk mixture. The interFoam solver we use is widely validated for applications like dam break events. Within the interFoam solver family, the interMixingFoam solver subdivides one of the phases into a two-phase mixture, a concept that may be seen viewed as an "equivalent fluid" approach but it goes beyond that due to the incorporation of concentration gradients. We demonstrate in figure 5 that our solver is able to simulate three-phase flows as accurately as drag-force-based multi-phase solvers with momentum exchange. We modified the manuscript to clearly explain the limitation of phase interactions and the corresponding motivation.

Referee #2 *points out that there is not one reference in the introduction to related earlier work, but only unproven statements of the authors, and he strongly recommends to re-write the introduction including recent work on modeling the constitutive flow behavior of grain-fluid mixtures.*

In the revised manuscript, we aim to clearly point out that the motivation of the model presented is its application for natural hazards protection rather than the detailed simulation of grain-fluid mixtures. We therefore include previous models in the beginning of the modeling approach description where we now include the work of Bohorquez (2008) as an example for modeling grain-fluid mixtures with a VOF approach. In general, we moved parts of the literature review to the accompanying paper to become part of a detailed discussion section that embeds the validation results.

Referee #2 *asks for a definition of interactions between a granular flow and a viscous force.*

We now mention the drag force and pore pressure as examples.

Referee #2 *recommends to be more cautious with using the term "viscous".*

In the revised manuscript we either use the term "fluid" or "visco-plastic".

Referee #2 *does not see the connection between the statement "the coupling between driving forces, topography and three dimensional flow-dependent internal friction can be addressed for each phase separately, accounting for the fundamental differences in flow mechanisms of granular and visco-plastic fluid flow" and Figure 1.*

We now state more precisely: "the fundamental differences in flow mechanisms of granular and visco-plastic fluid flow that arise from the presence or absence of Coulomb friction" and in Figure 1 we now point out that the Coulomb friction is part of the viscosity distribution shown for the gravel phase of the release body.

Referee #2 *wonders about the effect of buoyancy and excess fluid pressure in our model.*

Due to our phase-averaged approach, excess fluid pressure can't be modeled. Buoyancy is affecting cells of different density and affects the gravel phase and the fluid phase if they are initialized in separate regions like in Fig. 5.

In our presentation of the gravel phase rheology, ***Referee #2*** *questions how we know that the shear thinning fluid behavior of the fluid is important for flow resistance and if it is as important as the flow resistance of the grains.*

We now state that the dominant role of the shear thinning during high-speed flow is a feature of our model.

Referee #2 *wonders if the pressure p is the effective normal stress experienced only by the grains, or the bulk total normal stress?*

The pressure p is derived from the phase-averaged flow field and the phase-averaged densities. The question of the influence of effective fluid density is an interesting point. In our model we do not exclude a fluid pressure from the stress carried by the granular phase. This may only be valid for interstitial fluid of small viscosity and therefore is part of our limitation to flows where the drift flux can be neglected.

Referee #3:

SUMMARY REMARKS

As a preface to my comments I will disclose that I reviewed this paper because I was asked to review its companion paper (part 2: model validation). I felt that it was necessary to have a firm understanding of the first paper (part 1: model description) in order to understand the second. Consequently, I decided to review paper 1 as well as paper 2. However, after reading paper 1, I still lack a firm understanding of the authors' model. The paper provides an unsatisfying "model description" because it presents neither derivations of the model equations nor much in the way of data to support them. Instead, it presents a brief summary of the equations and a qualitative description of the computational strategy used to solve the equations. It would be more satisfying to see a precise derivation of the model equations as well as illustrations of how they're constrained by data. As it stands, the paper leaves much room for doubt about how the model actually works. My comments below elaborate this view.

General Response: The intention of the paper was not to derive new equations of motion to describe the debris-flow process, but rather to combine existing theory and discretizations with a well-known numerical solver. As part of this work we had to make some optimizations and modifications to the solver, however we emphasize that we did not change the underlying equations. For this reason, we prefer to rely on previously published arguments on the validity of the equations (Berberovic et al. 2009, Hoang et al. 2012, Deshpande et al. 2012, Haensch et al.

2013), rather than repeating existing validations. We regret that this was not fully apparent in the original manuscript, and we therefore have focused on making this clearer in the revised manuscript.

The numerical model is well validated (citations in the manuscript) for describing two-phase flows of immiscible and incompressible fluids. A subset of this so-called InterFoam solver family treats one of the immiscible phases as a mixture of two fluids. In our model these two 'fluids' are the granular sediment and the interstitial fluid. At the moment the solver describes this mixture of fluids as a complex rheology (another phase accounts for the immiscible air phase). The solver architecture is setup in a way that allows the composition to evolve, which will permit diffusion and phase separation in future releases. Therefore we prefer to present this as a strongly-coupled two-phase model.

COMMENTS ON MODEL EQUATIONS' INCONSISTENCIES

I'm perplexed by several mathematical attributes of the model. Parts of it appear to be internally inconsistent.

The text characterizes the model as "multiphase," and the forms of equations (13) through (16) (eq. (1) to (9) in the revised manuscript) *do indeed imply that the concentrations of different mixture constituents can evolve during transport. (Evolution of constituents' concentrations is a central feature of the continuum theory of multiphase mixtures.) Yet elsewhere in the text and equations, the velocities of all constituents are treated as identical, and dispersion of constituents by diffusion or other means is explicitly neglected. Thus, I can find no evidence of any physical process that would allow the concentrations of different constituents to evolve. As a result, it appears that the model is not really a multiphase mixture model but is instead a one-phase model that calculates the behavior of a fluid with an evolving free upper surface but with a fixed composition and complex rheology described by equations (1) through (9)* (eq. (16) to (27) in the revised manuscript). *The authors should either clarify or refute this key point. (I will also mention that a 50-year history exists of using complex, nonlinear rheological models to simulate the behavior of single-phase debris flows. Much of the research community has abandoned such models in favor of mixture models that simulate interactions of solid and fluid phases with evolving concentrations.)*

Yes, the equations are written in a general way to permit phase evolution to account for inter-phase momentum exchanges in future developments of the solver. However, in the basic method we presented we constrain the momentum exchange of the individual phases to always remain small to avoid violating the inter-phase momentum exchange relation.

Two approaches have been commonly used in the 50+ year history of non-Newtonian rheological debris-flow modeling: pressure-dependent rheologies accounting for grain collisions and shear dependent rheologies for viscous fluids. One novel part of our manuscript is to combine the two using a modern representation of each phase and a way to solve the equations. One interesting feature of this combined rheological approach is that it may be possible to explain much of the rheological behavior using only one free parameter. We lack the resources to explicitly test this hybrid rheology in the laboratory, however we show the applicability in the companion paper. We have attempted to make this point more clearly in the manuscript.

If the authors' model somehow does allow for differential advection of constituents with different densities, then this advection prohibits the use of a single momentum-conservation equation for the mixture as a whole (i.e., the authors' equation (10)) (eq. (14) in the revised manuscript). *(One cannot calculate the evolving momentum of a multiphase mixture by simply summing the momenta of the phases, because the nonlinear advective acceleration terms in the momentum-conservation equations for each phase do not sum to yield the advective acceleration of a mixture whose density is the concentration-weighted sum of the densities of the constituents. See, for example, Iverson, "The physics of debris flows," Reviews of Geophysics, 1997).*

We agree with Dr. Iverson that one cannot calculate the momentum of an evolving mixture simply by summing the momenta of the individual phases. We are grateful for this clear statement of the underlying problem! However, we have to point out that the phases in the model presented in this manuscript cannot change in composition, so in a strict sense our approach does not require a solution to this momentum-evolution problem. However, we would prefer to highlight this problem as a non-validated assumption in our model. We added this cautionary note to the manuscript and we also point out that a solution based on the drift-flux method would be suitable.

Additionally, equation (10) includes no gravitational body force. Isn't such a force necessary to drive debris-flow motion?

We now include a more complete set of equations in the manuscript, clearly showing the gravitational driving force.

COMMENTS ON THE RHEOLOCIAL MODEL

Assuming that the authors' model is, indeed, a one-phase model that calculates the behavior of a homogeneous, constant-density fluid with a complex rheology described by equations (1) through (9), then issues exist concerning how the rheological model is presented. First and foremost, the complete rheological model should be written in an explicit form that shows how all components of the amalgamated mixture stress tensor are related to those of the mixture rate-of-deformation tensor. At present the rheological model is presented piecemeal, and several of the pieces have issues.

For example, why is equation (1) presented as a scalar equation? Isn't a frame-invariant vector-tensor form of the equation required in order to apply it in 3-D computations? The information provided by the authors is insufficient for me to try to guess how they've implemented equation (1) in 3-D. Thirty years ago I addressed a similar 3-D rheology problem involving nonlinear, pressure-dependent viscoplasticity (Iverson, "A constitutive equation for mass-movement behavior", J. Geology, 1985). I subsequently abandoned that approach as suitable for describing the behavior of debris flows and landslides, but the approach highlighted some issues concerning material frame invariance, which the authors do not address.

Some equations that are presented in vector-tensor form by the authors also have issues. For example, consider equation (6) (eq. 24 in the revised manuscript) *[…] in which T_s is defined as the Cauchy stress tensor, p as the normalized pressure, I as the identity tensor, as the*

kinematic viscosity, and D as the rate-of -deformation tensor. (To discover the definition of the "normalized" pressure, which is not provided by the authors, I had to consult the paper by Domnik and Pudasaini, 2012. That paper defines normalized pressure as pressure divided by density.) With these definitions in hand, equation (6) is dimensionally inhomogeneous and consequently invalid. (The inhomogeneity follows immediately from the fact that Ts has dimensions of M/LT2, p has dimensions of L2/T2, vs has dimensions of L2/T, and D has dimensions of 1/T.) It appears that what the authors intended was for Ts also to be "normalized" by dividing it by the density, but their paper mentions neither this definition nor the formal definition of p. Instead, as a reader, I've had to decipher the authors' intent through my own detective work.

Another issue with equation (6) is that Ts must be a stress deviator tensor, and not the full "normalized" Cauchy stress tensor. This distinction is evident from the fact that the isotropic stress component pI has been isolated from Ts. With this interpretation, equation (6) is precisely the standard constitutive equation for an incompressible Newtonian fluid with a rate-and state dependent kinematic viscosity, which is defined in equation (9). It would be helpful for the authors to explain, in physical terms, why they believe that stresses within a deforming granular material can be accurately modeled using this approach. A comparison with data would be especially helpful. (Merely citing precedents of usage in other papers places the burden of seeking an explanation on the shoulders of readers, which is unfair. In scientific literature, the burden of explanation should be borne by authors, not by readers.)

The physical idea behind equation (6) (eq. 24 in the revised manuscript) is the introduction of a pressure-dependent energy dissipation. The model we chose is a stable pressure-dependent rheology which has already been applied to debris flows (Domnik & Pudasaini 2013). We tried the 3-parameter model of Forterre & Pouliquen (2008), but it was less stable with our solver. The solver presented does not model inter-phase momentum exchange and grain collisions and we justify the simplifications with the damping effect of the interstitial fluid. The model is not applicable to granular flow which makes it difficult to apply it to standard test cases. Coulomb-friction is part of the chosen approach of the rheology model of (Domnik & Pudasaini 2013). Actually the authors do not believe that the stresses within a granular material can be accurately modeled using this Coulomb-viscoplastic rheology. Instead we prefer to present this as a modern way to introduce pressure dependency based on the granular proportion. This is not explicitly tested in this manuscript, rather we demonstrate the plausibility for viscous mixtures in the companion paper. The inhomogeneity in dimensions resulted from not mentioning the dimension of the model parameter m_y due to the corresponding notation in (Domnik & Pudasaini 2012). It was implemented with the dimension time (OpenFOAM does not allow calculations with inconsistent dimensions) and the notation in the revised manuscript was altered accordingly.

Another mathematical issue appears in equations (7) and (9) (eq. (25) and (27) in the revised manuscript). *Those equations employ the function* $\exp(-m_y D)$ *, where* m_y *is a pure number that the authors set equal to 2, and*

$|D| = [2\,tr(D^2)]^{1/2}$ $|D| = [2\,tr(D^2)]^{1/2}$ *is a norm of the deformation-rate tensor. The authors fail to clarify why this particular norm provides an appropriate gauge of the magnitude of*

the tensor (as other scalar norms and tensor invariants of D also exist), but in any case the physical dimensions of D are the same as those of D, and are equal to 1/T. This constraint indicates that exp($-m_y D$) is an invalid mathematical operation, because mathematical functions can operate only on pure numbers, and not on quantities with physical dimensions. (As an aside, a rate-of-deformation tensor is not the same as a "strain rate" tensor, yet the authors use the terms interchangeably when referring to D. See the classic continuum mechanics text by L.E. Malvern for a detailed clarification of this point.)

We regret that we didn't explain what we meant by 'normalized' (it is normalized by density), and we also now realize that we were imprecise in the naming of stress deviator tensor in Equation 6. Furthermore, D is the strain rate tensor and my has the unit [s]. We corrected the unit issue in the manuscript accordingly, and we changed to non-normalized notations for clarity. This change, combined with the other changes described above, involved extensive re-writing of the equations: Instead of an imprecise and general introduction into the Finite Volume Method we now present the governing equations step by step in the form as applied in the model. We now first introduce the volumetric phase fractions to be able to initially present the continuity equation together with a transport equation and a momentum equation (eq. (3) to (5) in the revised manuscript) in the first subsection of the modeling approach. We then describe in detail how the transport and momentum equations are applied in our model and we provide a detailed set of equations governing the solution algorithm in an appendix, where it is shown how the divergence-free velocity field is found based on the momentum equation in an iterative procedure.

- Eq. (6), (7) and (9) are reformulated as eq. (24), (25) and (27) using the dynamic viscosity
- The density-normalized pressure is replaced by the pressure and is divided by density in equations 6 (now 24) and 9 (now 27)
- The momentum equation (10, now 5 and 14) is not divided by density and includes the source terms gravity and surface tension.
- The discretization of the momentum equation and the implementation of the solution procedure based on Issaa (1986) is now described in detail in the appendix.

OTHER COMMENTS KEYED TO PAGE NUMBERS

On p. 6352 the authors note that they employ linear averaging of concentration-weighted phase viscosities in order to obtain an effective viscosity for the mixture. It would be helpful to see a formal mathematical demonstration of this averaging procedure that includes all components of the 3-D stress tensor.

We rewrote the corresponding section accordingly. In the revised manuscript we introduce the deviatoric viscous stress tensor T with the momentum equation (5) and then show the relation to the phase-averaged dynamic viscosity μ in eq. (12) as

$$T = 2\mu D - \frac{2}{3}\mu(\nabla * U)I.$$

We then present the phased averaged viscosity as the sum of concentration-weighted contributions in eq. (13).

On p. 6359 the authors advocate use of 3-D rather than depth-averaged models on the basis of improved fits to data from dam-break experiments. However, few if any natural debris flows begin with dam breaks that impose large instantaneous force imbalances. Instead, debris flows generally arise from small perturbations to statically balanced initial states. This observation motivates a key question: how does the authors' model compute the initial stages of motion of a debris flow triggered by a small stress-state perturbation such as a pore-water pressure perturbation? Because their model takes no account of solid-fluid drag, it may be incapable of representing this effect. Yet this type of scenario is far more prevalent in nature than is a sudden dam break.

We include a large-scale natural debris flow release, the Johnson Landing Landslide Hazard of July 2012, in the validation work in the companion paper to illustrate the applicability and limitations, and we aim to model the irrigation-triggered shallow landslide experiment of Rüdlingen (Brönnimann 2011). The user can reset phase concentrations locally using the setFields utility of OpenFOAM, which would allow one to perform a stepwise increase in liquid phase concentrations within chosen parts of the release body to investigate the effect of infiltration. Besides that, the user could alter the water content of the liquid phase. However, we agree that the transition from a state of rest to phase mobilization due to solid-fluid drag cannot be accounted for in the present solver. We now explicitly state that we do not address the initiation issue in the manuscript.

On pages 6365-6367 the Discussion section begins with a literature review rather than a discussion of the authors' results. It then transitions to a brief description of findings from some test computations. Neither of these topics is addressed thoroughly, and neither really constitutes "discussion" material, in my view. Generally a discussion section follows a presentation of results, but the authors' paper lacks a "results" section.
On p. 6368 the Conclusions section states that, "… we have developed a debris flow model whose parameters can be estimated directly from the site geometry and material composition, rather than from extensive calibration." This is a strong statement that is not supported by the evidence presented in the paper.

We limited the corresponding statement and it will be moved to the companion paper where we can explore the range of validity of this statement using specific examples. Within the context of the validation experiments, we aim to highlight that the model is valuable in complex geometries on a local scale and that it cannot yet reproduce the evolution in material compositions that appears over longer distances, e.g. grain size sorting and the formation of granular fronts and viscous tails.

Manuscript prepared for Geosci. Model Dev.
with version 2014/09/16 7.15 Copernicus papers of the LaTeX class copernicus.cls.
Date: 31 January 2016

DebrisInterMixing-2.3: A finite volume solver for three dimensional debris flow simulations based on a single calibration parameter. Part one: Model description

A. v. Boetticher[1,3], J. M. Turowski[2,3], B. W. McArdell[3], D. Rickenmann[3], and J. W. Kirchner[1,3]

[1]Department of Environmental Systems Science, ETH Zentrum, CHN H41, 8092 Zürich, Switzerland
[2]Helmholtz-Centre Potsdam GFZ German Research Center for Geosciences, Telegrafenberg, 14473 Potsdam, Germany
[3]Swiss Federal Research Institute WSL, Zürcherstrasse 111, 8903 Birmensdorf, Switzerland

Correspondence to: Albrecht v. Boetticher (albrecht.vonboetticher@usys.ethz.ch)

Abstract. Here we present a three-dimensional fluid dynamic solver that simulates debris flows as a mixture of two fluids (a Coulomb-Viscoplastic model of the gravel mixed with a Herschel-Bulkley representation of the fine material suspension) in combination with an additional unmixed phase representing the air and the free surface. We link all rheological parameters to the material composition, i. e., to water content, clay content and mineral composition, content of sand and gravel, and the gravel's friction angle; the user must specify only a single free model parameter. The Volume-of-Fluid (VOF) approach is used to combine the mixed phase and the air phase into a single cell-averaged Navier-Stokes equation for incompressible flow, based on code adapted from standard solvers of the Open-Source CFD software OpenFOAM. The VOF method saves computational costs compared to drag-force based multiphase models. Thus depth-averaging is not necessary and complex three-dimensional flow structures can be simulated while accounting for the pressure- and shear-rate-dependent rheology.

1 Introduction

Debris flows typically occur in steep mountain channels. They are characterized by unsteady flows of water together with different contents of clay, silt, sand, gravel, and larger particles, resulting in a dense and often rapidly moving fluid mass. They are often triggered by heavy rainfall and can cause massive damage (Petley et al., 2007; Hilker et al., 2009). Their importance has increased due to intense settlement in mountainous regions and also due to their sensitivity to climate change

(Guthrie et al., 2010). Their damage potential is not limited to direct impact; severe damage can also be caused by debris flows blocking channels and thus inducing over-topping of the banks by subsequent flows.

Modeling debris flows is a central part of debris-flow research, because measuring the detailed processes in debris-flow experiments or in the field is challenging. It is still uncertain how laboratory tests can be scaled to represent real flow events, and the inhomogeneous mixture of gravel and fine material brings about interactions of granular flow and viscous forces like drag and pore-pressure that are difficult to track with the present measurement techniques at reasonable cost. As a consequence, the rheological behavior of debris flow material is incompletely understood.

Typically, current numerical modeling approaches cannot predict run-out distances or impact pressures of debris flows in known terrain without prior parameter calibration, based on simulating previous well-documented events that happened at the same site. This clearly represents a challenge in practical applications, because reliable calibration data are rarely available. In addition, the interactions between the granular and fluid phases, and the dynamic change in granular and fluid concentrations during the flow process, limit simple models to the narrow range of simulations that they have been calibrated for, where the fitted parameters account for these interactions. Complex models such as depth-averaged fluid simulations coupled to three dimensional particle methods are associated not only with high computational costs but also with a large number of model parameters, making model calibration the key issue for application to specific cases. This limits the possibilities of using debris flow models as a valid standard application in practice, because the user's ability to estimate values of poorly constrained parameters influences the results.

Here, we present an improved multiphase modeling approach as an alternative. We provide a coarse but effective solution linking the rheological model of the debris-flow material to field values such as grain size distribution and water content. The approach aims to link the knowledge of field experts for estimating the release volume and material composition with recent advances that account for complex flow phenomena using three-dimensional computational fluid dynamics. The parameters of the two resulting rheology models for the two mixing fluids are linked to material properties such that the model setup can be based on material samples collected from the field, yielding a model that has only one free parameter for calibration. One mixing phase represents the suspension of finer particles with water (also simply called slurry in this paper) and a second mixing phase accounts for the pressure-dependent flow behavior of gravel. A third gas phase is kept unmixed to model the free surface. The focus is on the flow and deposition process and the release body needs to be user-defined. Although, some aspects of material mobilization can be addressed by locally altering the concentration of the slurry phase and the water content of the slurry defined in the material properties, this is not within the scope of this paper.

Table 1. Nomenclature

α	phase fraction
α_m	fraction of the debris mixture (slurry + gravel)
$\boldsymbol{U}$	velocity
$\boldsymbol{Uc}$	inter-facial compression velocity
t	= time
$\mathbf{T}$, $\mathbf{T_s}$	deviatoric viscous stress tensor (s for granular phase)
$\mathbf{D}$	strain rate tensor
ρ	phase-averaged density, $\rho_i(i = 1, 2, 3)$ density of phase i, ρ_{exp} is a bulk density in experiment
p, p_d	pressure resp. modified pressure
D_{diff}	diffusion constant
ϕ	volumetric flux (ϕ_ρ denotes mass flux, ϕ_r a surface-normal flux)
$\mathbf{I}$	identity matrix
μ	phase-averaged dynamic viscosity, $\mu_i(i = 1, 2, 3)$ viscosity of phase i
μ_0	maximal dynamic viscosity
μ_{min}	minimal dynamic viscosity
μ_s	Coulomb-viscoplastic dynamic viscosity
∇	gradient
σ	free surface tension coefficient
κ	free surface curvature
$\boldsymbol{g}$	gravitational acceleration
τ	shear stress
τ_y	yield stress of slurry phase (τ_{y-exp} is a measured yield stress)
k	Herschel-Bulkley consistency factor
n	Herschel-Bulkley exponent
$\dot{\gamma}$	shear rate
C	volumetric solid concentration
P_0	volumetric clay concentration
P_1	reduced P_0 in case of high clay content
τ_{00}	free model parameter (affects slurry phase rheology)
τ_0	modified τ_{00} in case of high C
τ_{0s}	yield stress of granular phase modeled with Coulomb friction
β	slope angle
δ	internal friction angle approximated as angle of repose
m_y	constant model parameter (would affect gravel phase rheology)

2 Modeling approach

The debris flow material can be subdivided into a combination of a granular phase mixed with an interstitial fluid composed of the fine material suspension. The latter was successfully modeled in the past as a shear-rate dependent Herschel-Bulkley fluid (Coussot et al., 1998). Because pressure and shear drive the energy dissipation of particle-to-particle contacts, the shear rate substantially influences the energy dissipation within the granular phase. While the two-phase models of Iverson and Denlinger (2001) and Pitman and Le (2005) treated the granular phase as a shear-rate independent Mohr-Coulomb plastic material, dry granular material has been successfully modeled as a viscoplastic fluid by Ancey (2007), Forterre and Pouliquen (2008), Balmforth and Frigaard (2007) and Jop et al. (2006). We follow the suggestions given by Pudasaini (2012) to account for the non-Newtonian behavior of the fluid and the shear- and pressure-dependent Coulomb-viscoplastic behavior of the granular phase, as applied by Domnik et al. (2013). Several modeling approaches to account for the two-phase nature of debris flows used depth-averaged Navier-Stokes equations for each phase coupled by drag models (eg. Bozhinskiy and Nazarov (2000), Pitman and Le (2005), Pudasaini (2012) and Bouchut et al. (2015)). We apply the numerically more efficient method of Iverson and Denlinger (2001) and treat the debris flow material as one mixture with phase-averaged properties described by a single set of Navier-Stokes equations. The resulting reduction in numerical costs allows us to model the three-dimensional momentum transfer in the fluid as well as the free-surface flow over complex terrain and obstacles.

Multiphase flows of gas, fluid and sediment can be addressed with the so-called mixture- or drift-flux model in cases where the local difference in phase velocities is small (Bohorquez, 2008). The properties of all phases are cell-averaged to derive a single mass continuity and momentum balance equation describing the entire mixture. The model presented here has to be seen as a first step, assuming that the local velocity of the gravel is about the same as the velocity of the surrounding fluid, thus allowing us to neglect the drift-flux. This assumption would not be valid for debris flows with little interstitial fluid, or with interstitial fluid of small viscosity (i. e., a slurry with low concentrations of fine material). The assumption of equal velocities of both phases in one cell leads to a constant composition of the mixture by means of phase concentrations over the entire flow process. This basic model can be seen as a counterpart to the mixture model of Iverson and Denlinger (2001), extended by resolving the three dimensional flow structure in combination with a pressure- and shear-rate-dependent rheology linked to the material composition. In future work, we aim to relax the constraint of equal phase velocities and allow dispersion of constituents by introducing relative velocities of the gravel phase with respect to the fine sediment suspension according to Bohorquez (2012) and Damián (2013) together with a coupled Lagrangian particle simulation that can account for larger grains. The basic model presented here focuses on the role of pressure-dependent flow behavior of the gravel, in combination with the shear-dependent rheology of the slurry.

We base our model concept on the well-established finite volume solver interFoam, which is designed for incompressible two-phase flow simulations of immiscible fluids (Deshpande et al., 2012). A standard extension named interMixingFoam introduces two mixing phases without momentum exchange coupled to a third unmixed phase by surface tension. Numerical costs are kept reasonable due to the Volume-of-Fluid (VOF) method (Hirt and Nichols, 1981), which solves only one Navier-Stokes equation system for all phases. The viscosity and density of each grid cell is calculated as a concentration-weighted average between the viscosities of the phases that are present in the cell. Between the two mixing phases of gravel and slurry, the interaction reduces to this averaging of density and viscosity. In this way, the coupling between driving forces, topography and three dimensional flow-dependent internal friction can be addressed for each phase separately, accounting for the fundamental differences in flow mechanisms of granular and visco-plastic fluid flow that arise from the presence or absence of Coulomb friction (Fig. 1). We apply linear concentration-weighted averaging of viscosities for estimating the bulk viscosity of a mixture for simplicity. Non-linear averaging of viscosity between phases as suggested by Gao and Li (2012) may be introduced in the future.

2.1 Governing Equations

Assuming isothermal incompressible phases without mass transfer, we separate the modeled space into a gas region denoting the air and a region of two mixed liquid phases. The VOF method used here determines the volume fractions of all phases in an arbitrary control volume by using an indicator function which yields a phase fraction field for each phase. The phase fraction field represents the probability that a phase is present at a certain point in space and time (Hill, 1998). The air fraction may be defined in relation to the fraction of the mixed fluid α_m as

$$\alpha_1 = 1 - \alpha_m \tag{1}$$

and the mixed fluid α_m may be defined as the sum of the constant fractions of the mixing phases α_2 and α_3:

$$\alpha_m = \alpha_2 + \alpha_3. \tag{2}$$

The flow is defined by the continuity equation together with the transport and momentum equations:

$$\nabla \cdot \boldsymbol{U} = 0, \tag{3}$$

$$\frac{\partial \alpha_m}{\partial t} + \nabla \cdot (\boldsymbol{U} \alpha_m) = 0, \tag{4}$$

and

$$\frac{\partial(\rho \boldsymbol{U})}{\partial t} + \nabla \cdot (\rho \boldsymbol{U} \times \boldsymbol{U}) = -\nabla p + \nabla \cdot \mathbf{T} + \rho \boldsymbol{f}, \tag{5}$$

where $\boldsymbol{U}$ represents the velocity field shared by all phases, $\mathbf{T}$ is the deviatoric viscous stress tensor, ρ is the phase-averaged density, p denotes pressure and $\boldsymbol{f}$ stands for body forces per unit mass like gravity.

An efficient technique of the VOF method is to convect the phase fraction field α_m as an invariant with the divergence-free flow field $\boldsymbol{U}$ that is known from previous time steps:

$$\frac{\partial \alpha_m}{\partial t} + \nabla \cdot (\boldsymbol{U} \alpha_m) + \nabla \cdot (\alpha_1 \boldsymbol{U_c}) = 0, \tag{6}$$

where t denotes time and $\boldsymbol{U_c}$ is an artificial inter-facial compression velocity acting perpendicular to the interface between the gas region and the mixed liquid phases. The method allows a reconstruction of the free surface with high accuracy if the grid resolution is sufficient (Berberović et al., 2009; Hoang et al., 2012; Deshpande et al., 2012; Hänsch et al., 2013). The details about the interface compression technique, the related discretization and numerical schemes to solve eq. 6 are given in Deshpande et al. (2012). However, to allow evolving phase concentrations between the mixing phases of the slurry α_2 and the gravel α_3 in future releases, our modified version of the interMixingFoam solver applies eq. 6 separately to each mixing phase including diffusion:

$$\frac{\partial \alpha_i}{\partial t} + \nabla \cdot (\boldsymbol{U} \alpha_i) - D_{diff} \nabla^2 \alpha_i + \nabla \cdot (\alpha_1 \boldsymbol{U_c}) = 0, \tag{7}$$

where $i = 2, 3$ denote the slurry and gravel phases and D_{diff} is the diffusion constant that is set to a negligible small value within the scope of this paper.

The discrete form of eq. 7 is derived by integrating over the volume V of a finite cell of a grid-discretization of the simulated space, which is done in the finite volume method by applying the Gauss Theorem over the cell faces. The advective phase fluxes $\phi_{1..3}$ are obtained by interpolating the cell values of α_1, α_2 and α_3 to the cell surfaces and by multiplying them with the flux ϕ through the surface, which is known from the current velocity field. To keep the air phase unmixed, it is necessary to determine the flux ϕ_r through the interface between air and the debris flow mixture, and to subtract it from the calculated phase fluxes $\phi_{1..3}$. Inherited from the original interMixingFoam solver (OpenFOAM-Foundation, 2016a), limiters are applied during this step to bound the fluxes to keep phase concentrations between 0 and 1. With known fluxes $\phi_{1..3}$, the scalar transport equation without diffusion for each phase takes the form

$$\frac{\partial}{\partial t} \alpha_i + \nabla(\phi_i) = 0. \tag{8}$$

Equation 8 is solved using first-order Euler schemes for the time derivative terms, as has been recommended for liquid column breakout simulations (Hänsch et al., 2013).

After solving the scalar transport equations, the complete mass flux ϕ_ρ from the updated volumetric phase concentrations is constructed:

$$\phi_\rho = \phi_1 \cdot \rho_1 + \phi_2 \cdot \rho_2 + \phi_3 \cdot \rho_3, \tag{9}$$

where $\rho_{1..3}$ denote the constant densities of the corresponding phases and $\phi_{1..3}$ are the corresponding fluxes.

Fig. 2 illustrates how the phase volume distributions α_1 (air), α_2 (slurry) and α_3 (gravel) are used to derive cell-averaged properties of the continuum.

The conservation of mass and momentum is averaged with respect to the phase fraction α of each phase. The density field is defined as

$$\rho = \sum_i \rho_i \alpha_i \tag{10}$$

where ρ_i denotes density of phase i and the density is assumed to be constant.

The deviatoric viscous stress tensor $\mathbf{T}$ is defined based on the mean strain rate tensor $\mathbf{D}$ that denotes the symmetric part of the velocity gradient tensor derived from the phase-averaged flow field:

$$\mathbf{D} = \frac{1}{2}[\nabla \boldsymbol{U} + (\nabla \boldsymbol{U})^T], \tag{11}$$

and

$$\mathbf{T} = 2\mu \mathbf{D} - \frac{2}{3}\mu(\nabla \cdot \boldsymbol{U})\mathbf{I}. \tag{12}$$

$\mathbf{I}$ is the identity matrix and μ is the phase-averaged dynamic viscosity, which is simplified in analogy to eq. 10 as the concentration-weighted average of the corresponding phase viscosities:

$$\mu = \sum_i \mu_i \alpha_i \tag{13}$$

The term $\nabla \cdot \mathbf{T}$ in the momentum equation 5 is decomposed as $\nabla \cdot (\mu \nabla \boldsymbol{U}) + \nabla \boldsymbol{U} \cdot \nabla \mu$ to ease discretization. The body forces $\boldsymbol{f}$ in the momentum equation account for gravity and for the effects of surface tension. The surface tension at the interface between the debris flow mixture and air is modeled as a force per unit volume by applying a surface tension coefficient σ. The momentum conservation including gravitational acceleration $\boldsymbol{g}$ and surface tension is defined in our model as:

$$\frac{\partial(\rho \boldsymbol{U})}{\partial t} + \nabla \cdot (\rho \boldsymbol{U} \times \boldsymbol{U}) = -\nabla p_d + \nabla \cdot (\mu \nabla \boldsymbol{U}) + (\nabla \boldsymbol{U}) \cdot \nabla \mu - \boldsymbol{g} \cdot \boldsymbol{x} \nabla \rho + \sigma \kappa \nabla \alpha_1 \tag{14}$$

where κ denotes the local inter-facial curvature and $\boldsymbol{x}$ stands for position. The modified pressure p_d is employed in the solver to overcome some difficulties with boundary conditions in multiphase flow simulations. In case the free surface lies within an inclined wall forming a no-slip boundary condition, the normal component of the pressure gradient must be different for the gas phase and the mixture due to the hydrostatic component ρg. It is common to introduce a modified pressure p_d related to the pressure p by

$$p_d = p - \rho \boldsymbol{g} \cdot \boldsymbol{x}. \tag{15}$$

The gradient of the modified pressure includes the static pressure gradient and contributions that arise from the density gradient as well as a body force due to gravity (Berberović et al., 2009).

Together with the continuity equation 3 for the multi-phase flow, eq. 14 allows us to calculate the pressure and gravity driven velocities. The corresponding discretization and solution procedure with the PISO (Pressure-Implicit with Splitting of Operators (Issa, 1986)) algorithm is provided in appendix A. In the following section we present the rheology models that define the viscosity components for eq. 13.

2.2 Rheology model for the fine sediment suspension

The viscosity of the gas phase, μ_1 is chosen constant. The introduction of two mixing phases is necessary to distinguish between the pressure-dependent flow behavior of gravel and the shear-thinning viscosity of the suspension of finer particles with water. The rheology of mixtures of water with clay and sand can be described by the Herschel-Bulkley rheology law (Coussot et al., 1998), which defines the shear stress in the fluid as:

$$\tau = \tau_y + k\dot{\gamma}^n \tag{16}$$

where τ_y is a yield stress below which the fluid acts like a solid, k is a consistency factor for the viscosity of the sheared material, $\dot{\gamma}$ is the shear rate and n defines the shear-thinning ($n < 1$) or shear-thickening ($n > 1$) behavior. In OpenFOAM, the shear rate is derived in 3D from the strain rate tensor $\mathbf{D}$:

$$\dot{\gamma} = \sqrt{2 \cdot \mathbf{D} : \mathbf{D}} \tag{17}$$

The shear rate is based on the strain rate tensor to exclude the rotation velocity tensor that does not contribute to the deformation of the fluid body. The model can be rewritten as a generalized

Newtonian fluid model to define the shear-rate-dependent effective kinematic viscosity of the slurry phase as:

$$\mu_2 = k|\dot{\gamma}|^{n-1} + \tau_y|\dot{\gamma}|^{-1} \tag{18}$$

if the viscosity is below an upper limit μ_0 and

$$\mu_2 = \mu_0 \tag{19}$$

if the viscosity is higher, to ensure numerical stability.

With $n = 1$ the model simplifies to the Bingham rheology model that has been widely used to describe debris-flow behavior in the past. It may be reasonable to imagine the rheology parameters to be dependent on the state of the flow. However, even with the implicit assumption that the coefficients are a property of the material and not of the state of the flow, the Herschel-Bulkley rheology law was rarely applied in debris-flow modeling due to the large number of rheology parameters. We avoid this problem by assuming the rheology parameters to be defined by measurable material properties as described below.

2.2.1 Determination of rheology model parameters based on material properties

Results from recent publications allow the reduction of the number of free Herschel-Bulkley parameters to one. If the coarser grain fraction is confined to the gravel phase, the Herschel-Bulkley parameters for the finer material can be linked to material properties as measured using simple standard geotechnical tests. According to Coussot et al. (1998), the exponent n can be assumed constant as $1/3$, and k can be roughly estimated as $b \cdot \tau_y$, where the constant $b = 0.3\mathrm{s}^{-\mathrm{n}}$ for mixtures with maximum grain-sizes < 0.4 mm (Coussot et al., 1998). An approach for estimating the yield stress τ_y based on water content, clay fraction and composition, and the solid concentration of the entire debris flow material was proposed by Yu et al. (2013) as:

$$\tau_y = \tau_0 C^2 e^{22(C \cdot P_1)} \tag{20}$$

where C is the volumetric solid concentration of the mixture, $P_1 = 0.7P_0$ when $P_0 > 0.27$ and $P_1 = P_0$ if $P_0 <= 0.27$, and

$$P_0 = C_{kaolinite+chlorite} + 1.3C_{illite} + 1.7C_{montmorillonite} \tag{21}$$

where the subscript of C refers to the volumetric concentration (relative to the total volume of all solid particles and water) of the corresponding mineral. The discontinuity of P_1 at a modified clay

concentration of $P_0 = 0.27$ is a coarse adjustment to a more-or-less sudden change observed in the experimental behavior.

For $C < 0.47$, τ_0 is equal to τ_{00} and otherwise τ_0 can be calculated by

$$\tau_0 = \tau_{00} e^{5(C-0.47)} \tag{22}$$

where τ_{00} is the remaining free parameter which we use to account for the grid size dependency of the shear rate (Yu et al., 2013). We recommend a value of $\tau_{00} = 30$ Pa as a starting point for calibration. Yu et al. (2013) compared this method of estimating the yield stress τ_y to experimental results they obtained from a set of 514 flume experiments with mixtures of water and clay with fine and coarse sand and less than 5 % gravel. They determined the yield stress by releasing the material mixture from a reservoir into an inclined channel of 0.2 m width and by increasing the inclination slightly until remobilization occurred after the material came to rest. The experimental yield stress τ_{y-exp} was then determined as:

$$\tau_{y-exp} = \rho_{exp} g h sin(\beta), \tag{23}$$

where ρ_{exp} is the density of the applied mixture, g the acceleration due to gravity, h the maximum accumulation thickness of the deposit, and β the slope inclination. In addition, they compared the calculated yield stress of eq. 20 with experimental yield stresses reported by a number of authors including Coussot et al. (1998) and Ancey and Jorrot (2001). Ancey and Jorrot (2001) used 2 mm and 3 mm glass beads in a kaolinite dispersion as well as fine sand-kaolinite-water mixtures. Up to yield stresses of about 200 Pa the yield stresses estimated by eq. 20 fit the observed ones well. Thus, the yield stresses of sand-clay mixtures with water can be estimated using eq. 20 based on the volumetric concentration of the debris in the water-solids mixture and based on the percentages of different clays in the fraction of fine material. Adjustments to the numbers for calculating P_0 may be necessary to account for the activity of other clays.

The remaining uncertainties concern our assumptions that n is constant at a value of $1/3$, and that k can be defined in such simple dependency to τ_y in the presence of coarser sand. Experiments seem to confirm that n increases in presence of coarser material (Imran et al., 2001), but further research is needed to quantify this effect. Remaitre et al. (2005) found n to vary from 0.27 to 0.36. Schatzmann et al. (803) used $n = 0.33$ to reproduce measured curves obtained with a mixture of 27.5 volumetric percent slurry with 30 % gravel where gravel grain-sizes ranged from 3 to 10 mm, and used $n = 0.5$ to fit the Herschel-Bulkley model to the experiment with 22.5 % slurry and 30 % gravel. Based on the laboratory scale experiments that are presented in v. Boetticher et al. (2015) we have chosen $n = 0.34$ to obtain the best fit for the simulation presented by large-scale debris-flow experiments.

2.3 Representation of gravel by a Coulomb-viscoplastic rheology

During acceleration and high-speed flow, the shear-thinning behavior of both the fluid and the granular phase dominate the viscosity in our model. However, pressure-dependent friction becomes important as soon as the material experiences high pressures, accompanied by reduction in shear due to decelerations caused by channel slope reduction. Flows of granular material could be modeled as viscoplastic fluids (Ancey, 2007; Forterre and Pouliquen, 2008; Balmforth and Frigaard, 2007; Jop et al., 2006) as cited by Domnik and Pudasaini (2012). Based on Ishii (1975), the granular stress deviator tensor $\mathbf{T_s}$ can be written as:

$$\mathbf{T_s} = -\frac{p}{\rho}\mathbf{I} + 2\mu_s\mathbf{D}, \tag{24}$$

where $p\mathbf{I}$ is the pressure times the identity matrix and μ_s is the corresponding dynamic viscosity, which was modeled by Domnik and Pudasaini (2012) as:

$$\mu_s = \mu_{min} + \frac{\tau_{0s}}{||\mathbf{D}||}[1 - e^{-m_y||\mathbf{D}||}], \tag{25}$$

where μ_{min} is a minimal dynamic viscosity, τ_{0s} is a yield stress, and $||\mathbf{D}||$ is the norm of the strain-rate tensor defined by the authors as:

$$||\mathbf{D}|| = \sqrt{2tr(\mathbf{D}^2)}. \tag{26}$$

In eq. 25, m_y is a model parameter with units of s which we will keep constant, for reasons outlined in the following section. Domnik et al. (2013) suggested replacing the yield stress by a pressure-dependent Coulomb friction, $psin(\delta)$ where δ is the internal friction angle:

$$\mu_3 = \mu_{min} + \frac{psin(\delta)}{\rho_3||\mathbf{D}||}[1 - e^{-m_y||\mathbf{D}||}] \tag{27}$$

Here, this Coulomb-viscoplastic rheology model is used to describe the gravel phase. The pressure- and shear-dependent viscosity is calculated in every cell with the corresponding local pressure p and strain-rate tensor $\mathbf{D}$ derived from the phase-averaged flow field.

2.3.1 Gravel phase properties

The Coulomb-viscoplastic rheology law developed by Domnik et al. (2013) includes two parameters: the friction angle δ, and the parameter m_y influencing the transition between yielded and unyielded regions. For smaller values of m_y, the transition is smoother. In the absence of shear, to achieve a viscosity representing a Coulomb friction equal to $p \cdot sin(\delta)$ where p is the local pressure, m_y needs

to be equal to 1 s. However, the development of μ_s under large pressure or strong shear is the same for both $m_y = 1$ s and $m_y = 0.2$ s, but parts of the nearly immobile material that face little pressure (in general, immobile material close to the surface) show a significant reduction in viscosity when $m_y = 0.2$ s (Fig. 3). As a consequence, m_y minimally affects debris flow release and flow at large scales, but material with a shallow flow depth in a run-out plane close to deposition may develop front fingering (which is dependent on, and sensitive to, the value of m_y) by allowing sudden local solidification. We choose m_y to be constant and equal to 0.2 s for all simulations.

For small friction angles, the modeled viscosity of the gravel phase decreases rapidly with increasing shear. Larger friction angles increase the viscosity and extend the pressure dependency to larger shear rates (Fig. 4). We estimated the friction angle δ based on the maximum angle of repose in tilt-table tests of the gravel. In our laboratory experiments, we determined the friction angle in a simple adaptation of the method of Deganutti et al. (2011) by tilting a large box with loose material until a second failure of the material body occurred.

In analogy to the Herschel-Bulkley implementation, an upper limit for the viscosity is implemented to maintain numerical stability. Pressure-dependent viscosity in the incompressible Navier-Stokes equations causes numerical instability as soon as the eigenvalues of the symmetric part of the local velocity gradient become larger than $1/(2(\delta\mu/\delta p))$. Following Renardy (1986), we locally limit the viscosity to keep it below a corresponding local stability limit.

3 Quality characteristics of the model

3.1 Effects of time step size on rheology

Because most debris-flow models are depth-averaged and use shallow-water approximations, one could ask why a three-dimensional approach is necessary. Brodani-Minussi and deFreitas Maciel (2012) compared dam-break experiments of a Herschel-Bulkley fluid and its numerical simulations using the VOF approach with published shallow-water-equation-based models. Especially for the first instant after the material release, the application of shallow-water equations seems to introduce errors that are propagated throughout the process, leading to erroneous run-out estimates. A similar problem arises when modeling debris-flow impacts on obstacles. Simulating the impact of material with velocity-dependent rheology that is kept constant over the time step although it actually changes with the changing flow leads to an accumulating over- or underestimation of energy dissipation. In our model, during release of immobile material that accelerates, the viscosity is overestimated over each time step. As a consequence, the velocity at the end of the time step is underestimated, which again amplifies the overestimation of viscosity in the next time step. Conversely, at an impact, the sudden deceleration causes an underestimation of viscosity over the time step length, leading to an overestimated velocity that again amplifies the underestimation of the viscosity in the next time step. As a result, flow velocities change with changing time step size. Avalanche codes such as

RAMMS (Christen et al., 2007) deal with this problem by calibrating the model to data from previous events at the same location and similar conditions. But changes in release volume or position can lead to different accelerations and corresponding changes in the automatic time step control can alter the development of rheology over time. As long as a flow stage is reached where the flow stops accelerating, the influence on the final front velocity should be negligible. Other debris flow models, which do not iteratively adjust viscosity, cannot accurately simulate impacts. Here, our model constitutes a significant improvement, since in the three-dimensional solver we presented, the viscosity bias was reduced by implementing a corrector step: taking the average between the viscosity at the beginning of the time step and the viscosity that corresponds to the velocity field at the end of the time step, the time step is solved again, leading to a better calculation of the velocity. This step can be repeated, according to user specifications, to correct the viscosity several times. Although this procedure increases numerical calculation time, it clearly reduces the time-step dependency of the simulation. Some dependency on the time step is still present when modeling the collapse of material columns, but the origin of this problem is different because it occurs also for Newtonian fluids.

3.2 Effect of grid resolution on rheology

Since the shear rate influences both viscosity models, a strong influence of grid resolution on viscosity results, because the shear rate is averaged over the cell size. For flows over rough topography this may be less critical, but for laboratory flume experiments with thin shear bands the results may depend on grid resolution. When simulating laboratory flume experiments where debris-flow material accelerated in a relatively narrow and short channel (Scheidl et al., 2013), a cell height of 1.5 mm, which is of the order of the laboratory rheometer gap, was still not fine enough to reach the limit of grid sensitivity. The free model parameter τ_{00} influences the shear-rate-dependent term of the visco-plastic rheology model and can be used to adjust the simulation to the grid resolution. As long as the gravel phase and grid resolution do not change, it should be possible to model different water and clay contents based on one calibration test. However, as the composition changes, both τ_y and τ_{00} must change commensurately, since a change in yield stress affects the shear rate. Our procedure for adjusting to different mixtures based on one calibrated test is to perform one iteration step for the yield stress of the new mixture; by calculating τ_y based on the original τ_{00} value from the calibration test but with the new material composition, an updated yield stress of the new mixture is determined. Raising or lowering τ_{00} by the same ratio as the change from the original yield stress of the calibration test to the updated yield stress generates the final τ_y as it is applied to the simulation of the new mixture.

The viscosity of the granular phase is averaged over the cell faces to avoid discontinuous viscosity jumps between cells, which may cause instability due to the sensitivity of incompressible solvers to pressure-dependent viscosity. However, thin cells that allow a precise calculation of the shear gra-

dient lead to a preferred direction of the smoothing of the granular phase's viscosity which may introduce physically unrealistic behavior. Cell length (in the flow direction), cell width and cell height should at least be of the same order. Especially when front fingering is of interest, a grid resolution test should be carried out, ensuring that front instability is not caused by a large aspect ratio of the cell dimensions.

4 Discussion

Because the purpose of this paper is to illustrate the solver structure and model basis, we defer a detailed discussion of model performance to the accompanying paper, in which the model is validated against laboratory tests, large scale experiments and natural hill-slope debris flow events. Here, we discuss only the efficiency of the solver itself, together with a general test about the model accuracy in a gravity-driven open channel flow. The lack of standard benchmark test cases for debris-flow solvers was the motivation to select a numerical test case to compare model speedup between our approach and a closely related drag-force-based Eulerian multiphase model, and to select a well-defined gravity-driven turbulent open channel flow experiment with clear water to inspect the solver validity.

In comparison to drag-force-based Eulerian multiphase models, the Volume of Fluid approach applied here provides significant reduction in calculation time. For an estimate we compared our model with the OpenFOAM standard solver multiphaseEulerFoam. We selected the official tutorial case damBreak4phaseFine, but turned the water phase into mercury to gain a three-phase test case, and applied the standard solver settings from the case to our model. On a CentOS 6.3 Linux machine with 31 GiB memory and sixteen Intel Xeon CPU E5-2665 @ 2.40 GHz processors, our model resulted in a 5.5 times faster calculation with a comparable collapse of the modeled mercury and oil columns (Fig. 5). For the sake of completeness our calculation included one iterative viscosity correction step, thus the model efficiency can be estimated to be about ten times higher than a drag-force-based phase coupling approach.

The model was also applied to an open clear water channel experiment with about 50.6 l/s discharge in a 40 m long and 1.1 m wide rectangular smooth channel with 0.026% inclination (Fischer, 1966). The slurry phase was initialized as water together with a zero gravel phase concentration. A Hybrid URANS-LES model was applied to account for the turbulent flow. Instead of an inlet discharge the model applied periodic inlet and outlet boundary conditions and the flow was driven by gravity. The debrisInterMixingFoam solver predicted the discharge of the turbulent channel flow with an underestimation of 15% and underestimated the corresponding surface elevation by 2.5%. However, the deviations in predicted and measured average flow velocities are probably related to shortcomings of the URANS turbulence model at the bottom boundary, as a comparison between a

measured and simulated vertical velocity profile suggests (Fig. 6). Due to the lack of a clearly defined benchmark test case for debris flow models, we have chosen this setup as a well-defined larger-scale laboratory test case where the solver faces varying modeled fluid viscosity due to turbulence.

5 Conclusions

The new debris-flow solver has two main strengths. First, it can model three-dimensional flows and their impact against complexly shaped objects, representing the processes at a high level of detail. Second, its design allows simulating different debris flow material compositions without recalibrating the one free parameter, as long as the simulation grid does not change. Due to the solver's pressure- and shear-dependent rheology, realistic deposit geometries and release dynamics can be achieved, as presented and discussed on the basis of test cases in the accompanying paper. By systematically excluding unknown parameters from the model architecture and by accounting for known flow phenomena in a simplified way, we have developed a debris flow model whose parameters can be roughly estimated based on material composition, leaving only a single calibration parameter. The concept is promising, however important parts of phase interactions are neglected in favor of lower numerical costs and shorter calculation times. The model is still limited to small simulations of several hundred square meters in surface area unless a powerful computer cluster can be used.

Appendix A: A

The following section describes the detailed implemetation of the PISO iteration procedure as described in Deshpande et al. (2012). By applying the continuum surface force model of Brackbill et al. (1992), the volume integral of eq. 14 is given as

$$\int_{\Omega_i} \frac{\partial \rho \boldsymbol{U}}{\partial t} dV + \int_{\partial\Omega_i} (\rho \boldsymbol{U}\boldsymbol{U}) \cdot \boldsymbol{n} dS = \\ -\int_{\Omega_i} \nabla p_d dV - \int_{\Omega_i} \boldsymbol{g} \cdot \boldsymbol{x} \nabla \rho dV + \int_{\Omega_i} \sigma \kappa \nabla \alpha_1 dV + \int_{\partial\Omega_i} (\mu \nabla \boldsymbol{U}) \cdot \boldsymbol{n} dS + \int_{\Omega_i} \nabla \boldsymbol{U} \cdot \nabla \mu dV. \quad \text{(A1)}$$

The computational domain is discretized into finite-volume cells. Each cell is considered as the owner of exactly one face that it shares with an adjacent neighbor cell, thus each face has a defined owner cell. A surface normal vector S_f with magnitude equal to the surface area of the face is defined on the face pointing outward from the owner cell (Fig. 7). The value at face f of any variable χ calculated in the cell centers as χ_P and χ_N (Fig. 7) can be derived by interpolation using a mixture of central and upwind schemes:

$$\chi_{\mathbf{f}} = \gamma(\chi_P - \chi_N) + \chi_N, \quad \text{(A2)}$$

with a weighting factor γ that can account for the flow direction based on the chosen interpolation scheme and flux limiter. In case of a linear interpolation scheme and a flux limiter ψ, γ can be defined as

$$\gamma = \psi \frac{fN}{d} + (1-\psi)\frac{\phi_f}{|\phi_f|}, \tag{A3}$$

where d is the distance between the cell centers P and N and fN is the distance from the face center to the cell center N. The face flux denoted as ϕ_f serves as a switch to account for the flow direction since it turns negative when the flow is from N to P (Berberović et al., 2009). Several limiters are implemented (OpenFOAM-Foundation, 2016b); we chose the vanLeer scheme and assumed uniform grid spacing to simplify the following explanations with $fN/d = 0.5$.

Variables that are evaluated at the cell faces are subscripted by f. Due to stability problems that arise from the pressure-velocity coupling in collocated meshes (Ferziger and Peric, 2002), the pressure is solved for the cell centers whereas the velocity is interpolated to the cell faces within the PISO loop.

With the switch function

$$\zeta(\phi_f) = \frac{\phi_f}{|\phi_f|} \tag{A4}$$

the velocity $\boldsymbol{U}_f$ at face f can be written based on eq. A2 and A3 as

$$\boldsymbol{U}_f = \frac{\boldsymbol{U}_P}{2}(1+\zeta(\phi_f)(1-\psi)) + \frac{\boldsymbol{U}_N}{2}(1-\zeta(\phi_f)(1-\psi)), \tag{A5}$$

and the corresponding face-perpendicular velocity gradient is given by Deshpande et al. (2012) as

$$\nabla^{\perp}{}_f \boldsymbol{U} = \frac{\boldsymbol{U_N} - \boldsymbol{U_P}}{|d|}. \tag{A6}$$

At the present time step t^n the phase averaged density of the next time step ρ^{n+1} is known from solving the transport equations. In a first approximation, the corresponding viscosity field μ^{n+1} can be derived accordingly. A simplified formulation of the momentum equation A1 without pressure, surface tension and gravity terms discretized for cell P could then be formulated as

$$\frac{(\rho^{n+1}\tilde{\boldsymbol{U}}) - (\rho^n \boldsymbol{U^n})}{\Delta t}|\Omega_P| + \sum_{f\in\partial\Omega_i} \rho^n{}_f \phi^n{}_f \tilde{\boldsymbol{U}}_f = \sum_{f\in\partial\Omega_i} \mu^{n+1}{}_f \nabla^{\perp}{}_f \tilde{\boldsymbol{U}} |\boldsymbol{S}_f| + \nabla \boldsymbol{U}^n \cdot \nabla \mu^{n+1} |\Omega_P|. \tag{A7}$$

The tilde stands for the velocity at cell P predicted in the current iterative step, for which eq. A7 yields an explicit expression. For that purpose, eq. A5 and A6 are inserted into eq. A7 using the

velocity of the prior iteration step, $\boldsymbol{U^m}$, in all neighbor cells (Deshpande et al., 2012). The explicit expression for the estimated velocity is

$$A_P\tilde{\boldsymbol{U}} = H(\boldsymbol{U^m}), \tag{A8}$$

and by including surface tension and gravity this leads to

$$\tilde{\boldsymbol{U}} = \frac{H(\boldsymbol{U^m})}{A_P} + \frac{\sigma\kappa\nabla\alpha_1^{n+1}}{A_P} - \frac{\boldsymbol{g}\cdot\boldsymbol{x}\nabla\rho}{A_P}. \tag{A9}$$

The detailed composition of $H(\boldsymbol{U^m})$ and A_P formulated with respect to the splitting between neighbor and owner cells can be found in Deshpande et al. (2012); here it is sufficient to keep in mind that $H(\boldsymbol{U^m})$ contains all off-diagonal contributions of the linear system.

The next step is to assemble the approximated face flux

$$\tilde{\phi_f} = \Big(\frac{H(\boldsymbol{U^m})}{A_P}\Big)_f \cdot \boldsymbol{S}_f + \Big(\frac{(\sigma\kappa)^{n+1}(\nabla^\perp{}_f\alpha_1)^{n+1}}{A_P}\Big)_f |\boldsymbol{S}_f| - \Big(\frac{(\boldsymbol{g}\cdot\boldsymbol{x})^{n+1}(\nabla^\perp{}_f\rho)^{n+1}}{A_P}\Big)_f |\boldsymbol{S}_f| \tag{A10}$$

where the subscript f indicates that the variable values at the faces are used. The final flux is found by adding the pressure contribution

$$\phi^{m+1}{}_f = \tilde{\phi_f} - \Big(\frac{\nabla^\perp{}_f p_d^{m+1}}{A_P}\Big)_f |\boldsymbol{S}_f|. \tag{A11}$$

The sum of the flux over the cell faces needs to be zero due to mass conservation for the incompressible flow

$$\sum_{f\in\partial\Omega_i} \phi^{m+1}{}_f = 0, \tag{A12}$$

Thus the pressure is defined by the linear equation system for the updated pressure ${p_d}^{m+1}$

$$\sum_{f\in\partial\Omega_i} \Big(\frac{\nabla^\perp{}_f p_d^{m+1}}{A_P}\Big)_f |\boldsymbol{S}_f| = \sum_{f\in\partial\Omega_i} \tilde{\phi_f}, \tag{A13}$$

and can be solved with the preconditioned conjugate gradient (PCG) algorithm, to mention one of several options implemented in OpenFOAM. With the updated pressure ${p_d}^{m+1}$, the face fluxes $\phi^{m+1}{}_f$ are derived from eq. A11 and the updated velocity filed $\boldsymbol{U}^{m+1}$ is obtained from the explicit velocity correction

$$\boldsymbol{U}^{m+1} = \tilde{\boldsymbol{U}} + \Big(\frac{1}{A_P}\Big)\Big(\sum_{f\in\partial\Omega_i} \frac{(\boldsymbol{S}_f\otimes\boldsymbol{S}_f)}{|\boldsymbol{S}_f|}\Big)^{-1} \bullet \Big(\sum_{f\in\partial\Omega_i} \Big(\frac{\phi^{m+1}{}_f - \tilde{\boldsymbol{U}}_f\cdot\boldsymbol{S}_f}{(\frac{1}{A_P})_f}\Big)\frac{\boldsymbol{S}_f}{|\boldsymbol{S}_f|}\Big) \tag{A14}$$

which is the end of the PISO loop. After updating the index m to $m+1$, the iteration restarts with recalculating H with the updated velocity from equation A8, repeating the loop until a divergence-free velocity field is found.

A1 Code availability

The source-code can be downloaded from the supplement application.zip. Please follow the instructions given in the README.pdf file for installation.

Acknowledgements. We thank Shiva Pudasaini, Johannes Hübl and Eugenio Oñate for thoughtful critiques and suggestions.

References

Ancey, C.: Plasticity and geophysical flows: a review., J. Non-Newton. Fluid Mech., 142, 4–35, 2007.

Ancey, C. and Jorrot, H.: Yield stress for particle suspensions within a clay dispersion., J. Rheol., 45, 297–319, 2001.

Balmforth, N. and Frigaard, I.: Viscoplastic fluids: from theory to application, J. Non-Newton. Fluid Mech., 142, 1–3, 2007.

Berberović, E., van Hinsberg, N. P., Jakirlić, S., Roisman, I. V., and Tropea, C.: Drop impact onto a liquid layer of finite thickness: Dynamics of the cavity evolution, Phys. Rev. E, 79, 036 306, doi:10.1103/PhysRevE.79.036306, 2009.

Bohorquez, P.: Study and Numerical Simulation of Sediment Transport in Free-Surface Flow, Ph.D. thesis, Universit"at Malaga, Spain, 2008.

Bohorquez, P.: Finite Volume Method of Falling Liquid Films Carrying Monodispersed Spheres in Newtonian Regime, AIChE J, 58, 2601–2616, 2012.

Bouchut, F., Fernandez-Nieto, E. D., Mangeney, A., and Narbona-Reina, G.: A two-phase shallow debris flow model with energy balance, ESAIM-MATHEMATICAL MODELLING AND NUMERICAL ANALYSIS-MODELISATION MATHEMATIQUE ET ANALYSE NUMERIQUE, 49, 101–140, 2015.

Bozhinskiy, A. N. and Nazarov, A. N.: Two-phase model of debris flow, in: 2nd International Conference on Debris-Flow Hazards Mitigation, pp. 16–18, Teipei, Taiwan, 2000.

Brackbill, J. U., Kothe, D. B., and Zemach, C.: A continuum method for modeling surface tension, J. Comput. Phys., 100, 335–354, 1992.

Brodani-Minussi, R. and deFreitas Maciel, G.: Numerical Experimental Comparison of Dam Break Flows with non-Newtonian Fluids, J. of the Braz. Soc. of Mech. Sci. and Eng., 34-2, 167–178, 2012.

Christen, M., Bartelt, P., and Gruber, U.: RAMMS - a Modelling System for Snow Avalanches, Debris Flows and Rockfalls based on IDL, Photogramm. Fernerkund. Geoinf., 4, 289–292, 2007.

Coussot, P., Laigle, D., Aratano, M., Deganuttil, A., and Marchi, L.: Direct determination of rheological characteristics of debris flow, J Hydraul Eng, pp. 865–868, 1998.

Damián, S. M.: An extended mixture model for the simultaneous treatment of schort and long scale interfaces, Ph.D. thesis, Universidad Nacional de Litoral, Argentina, 2013.

Deganutti, A., Tecca, P., and Genevois, R.: Characterization of friction angles for stability and deposition of granular material, in: Italian Journal of Engineering and Environment: 5th International Conference on Debris-Flow Hazards: Mitigation, Mechanics, Prediction and Assessment, pp. 313–318, Padua, Italy, 2011.

Deshpande, S. S., Anumolu, L., and Trujillo, M. F.: Evaluating the perfomance of the two-phase flow solver interFoam, Computational Science and Discovery, 5, 1–33, 2012.

Domnik, B. and Pudasaini, S.: Full two-dimensional rapid chute flows of simple viscoplastic granular materials with a pressure-dependent dynamic slip-velocity and their numerical simulations, J. Non-Newton. Fluid Mech, 173–174, 72–86, 2012.

Domnik, B., Pudasaini, S., Katzenbach, R., and Miller, S.: Coupling of full two-dimensional and depth-averaged models for granular flows, J. Non-Newton. Fluid Mech, 201, 56–68, 2013.

Ferziger, J. H. and Peric, M.: Computational Methods for Fluid Dynamics, Springer 3rd ed., Berlin, 2002.

Fischer, H. B.: Longitudinal Dispersion in Laboratory and Natural Streams, Ph.D. thesis, California Institute of Technology, 1966.

Forterre, Y. and Pouliquen, O.: Flows of dense granular media, Annu. Rev. Fluid Mech., 40, 1–24, 2008.

Gao, Y. and Li, K.: New models for calculating the viscosity of mixed oil, Fuel, 95, 431–437, 2012.

Guthrie, R., Mitchell, J., Lanquaye-Opoku, N., and Evans, S.: Extreme weather and landslide initiation in coastal British Columbia, Journal of engineering geology and hydrogeology, 43, 417–428, 2010.

Hänsch, S., Lucas, D., Höhne, T., Krepper, E., and Montoya, G.: Comparative simulations of free surface flows using VOF-methods and a new approach for multi-scale interfacial structures, in: Proceedings of the ASME 2013 Fluids Engineering Summer Meeting, Incline Village, Nevada, USA, 2013.

Hilker, N., Badoux, A., and Hegg, C.: The Swiss flood and landslide damage database 1972-2007, Nat. Hazards Earth Syst. Sci., 9, 913–925, 2009.

Hill, D.: The Computer Simulation of Dispersed Two-Phase Flows, Ph.D. thesis, Imperial College, University of London, 1998.

Hirt, B. and Nichols, B.: Volume of Fluid (VOF) Method for the Dynamics of Free Boundaries, Journal of Computational Physics, 39, 201–225, 1981.

Hoang, D., van Steijn, V., Kreutzer, M., and Kleijn, C.: Modeling of Low-Capillary Number Segmented Flows in Microchannels Using OpenFOAM, in: Numerical Analysis and Applied Mathematics ICNAAM 2012, AIP Conf. Proc., vol. 1479, pp. 86–89, Kos Island, Greece, 2012.

Hürlimann, M., McArdell, W., and Rickli, C.: Field and laboratory analysis of the runout characteristics of hillslope debris flows in Switzerland, Geomorphology, 232, 20–32, doi:10.1016/j.geomorph.2014.11.030, 2015.

Imran, J., Parker, G., Locat, J., and Lee, H.: 1D numerical model of muddy subaqueous and subaerial debris flows, J Hydraul. Eng., pp. 959–968, 2001.

Ishii, M.: Thermo-Fluid Dynamic Theory of Two-Phase Flow, Eyrolles, Paris, 1975.

Issa, R.: Solution of the implicitly discretized fluid-flow equations by operator-splitting, J Comp. Phys., 62, 40–65, 1986.

Iverson, R. and Denlinger, P.: Flow of variably fluidized granular masses across three-dimensional terrain: 1. Coulomb mixture theory, J. Geophys. Res., 106, 537–552, 2001.

Jop, P., Forterre, Y., and Pouliquen, O.: A constitutive law for dense granular flows, Nature, 441, 727–730, 2006.

OpenFOAM-Foundation: OpenFOAM Standard Solvers, Website User Guide of OpenFOAM, http://www.openfoam.org/docs/user/standard-solvers.php, visited 12.01.2016., 2016a.

OpenFOAM-Foundation: OpenFOAM Standard Schemes, Website User Guide of OpenFOAM, http://cfd.direct/openfoam/user-guide/fvSchemes/, visited 12.01.2016., 2016b.

Petley, D. N., Hearn, G. J., Hart, A., Rosser, N. J., Dunning, S. A., Oven, K., and Mitchell, W. A.: Trends in landslide occurence in Nepal, Nat Hazards, 43, 23–44, 2007.

Pitman, E. and Le, L.: A two-fluid model for avalanche and debris flows, Philos. Trans. R. Soc. A, 363, 1573–1602, 2005.

Pudasaini, S.: A general two-phase debris flow model, J. Geophys. Res., 117, F03 010, 2012.

Remaitre, A., Malet, J., Maquaire, O., Ancey, C., and Locat, J.: Flow behaviour and runout modelling of a complex derbis flow in a clay-shale basin, Earth Surf Proc Landforms, 30, 479–488, 2005.

Renardy, M.: Some remarks on the Navier-Stokes Equations with a pressure-dependent viscosity, Comm. in Partial Differential Equations, 11, 779–793, 1986.

Schatzmann, M., Fischer, P., and Bezzola, G. R.: Rheological Behavior of Fine and Large Particle Suspensions, J. Hydraul Eng.-ASCE, 796, 391–430, 803.

Scheidl, C., Chiari, M., Kaitna, R., Müllegger, M., Krawtschuk, A., Zimmermann, T., and Proske, D.: Analysing Debris-Flow Impact Models, Based on a Small Scale Modelling Approach, Surv. Geophys, 34, 121–140, 2013.

v. Boetticher, A., Turowski, J. M., McArdell, W. B., Rickenmann, D., Hürlimann, M., Scheidl, C., and Kirchner, J. W.: (submitted) DebrisInterMixing-2.3: A Finite Volume solver for three dimensional debris flow simulations based on a single calibration parameter. Part two: Model validation, Geoscientific Model Development, 2015.

Yu, B., Ma, Y., and Qi, X.: Experimental Study on the Influence of Clay Minerals on the Yield Stress of Debris Flows, J. Hydraul. Eng., 139, 364–373, 2013.

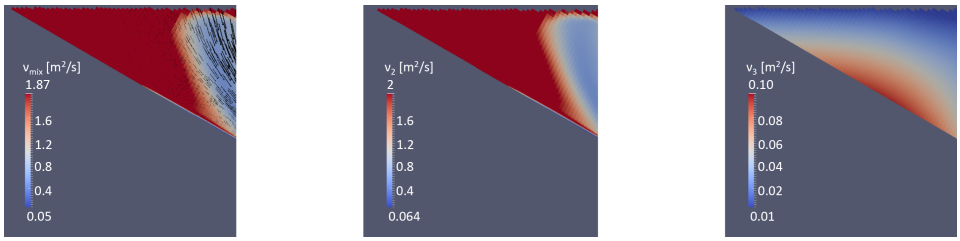

Figure 1. Viscosity distribution (indicated by color scale) along a 28 cm long section through the modeled 0.01 m^3 release block 0.2 s after release, corresponding to the experimental setup of Hürlimann et al. (2015). The starting motion (black velocity arrows) with corresponding viscosity distribution of the mixture (left) is a consequence of blending pure shear-rate dependent slurry-phase rheology (center) with the pressure- and shear-rate-dependent gravel phase rheology that accounts for Coulomb friction (right). Because the gravel concentration in this example is low, its effect on the overall viscosity is small.

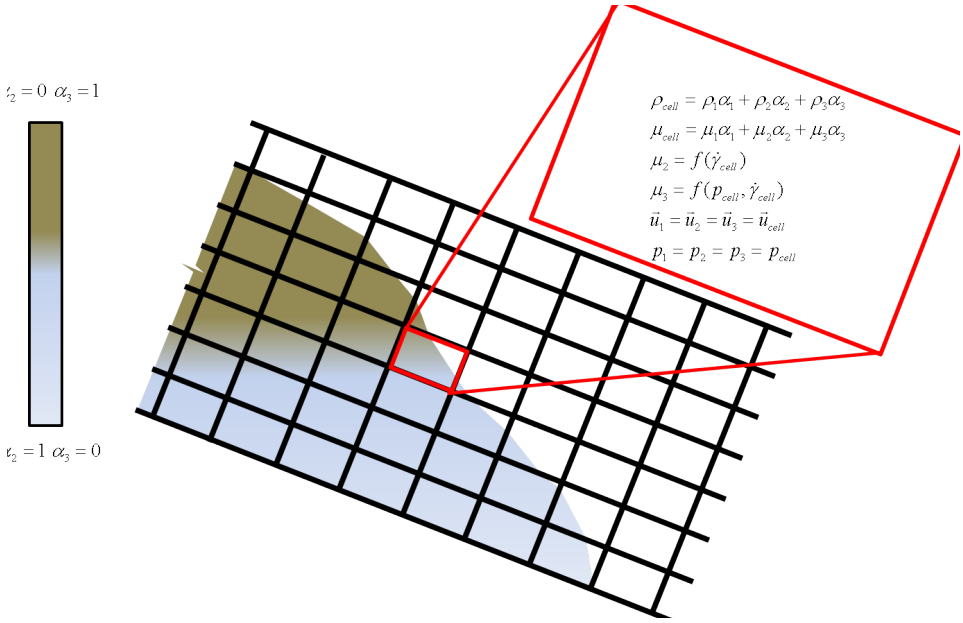

Figure 2. Longitudinal section through a debris flow front discretized with finite volume-cells, showing the constitutive equations for one cell with density ρ and viscosity μ given the densities $\rho_{1..3}$, viscosities $\mu_{1..3}$ and proportions $\alpha_{1..3}$ of phases present. 1 denotes air (white colored cell content), 2 the mud and 3 the gravel phase, respectively.

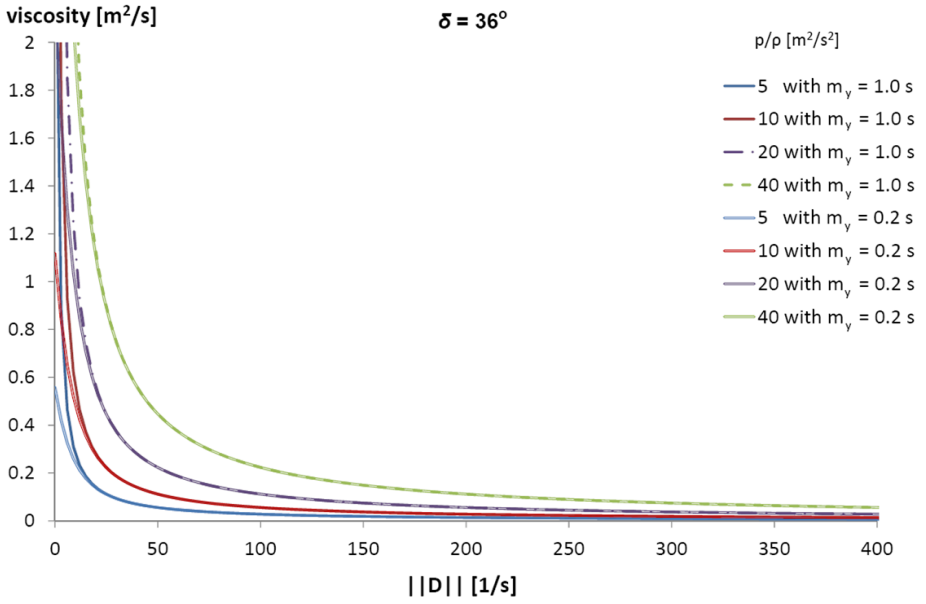

Figure 3. Dependency of the kinematic gravel phase viscosity ν_s (normalized by density) on the norm of the strain rate tensor $||D||$ at different levels of pressure normalized by density, for $m_y = 1$ s and $m_y = 0.2$ s and a friction angle $\delta = 36°$.

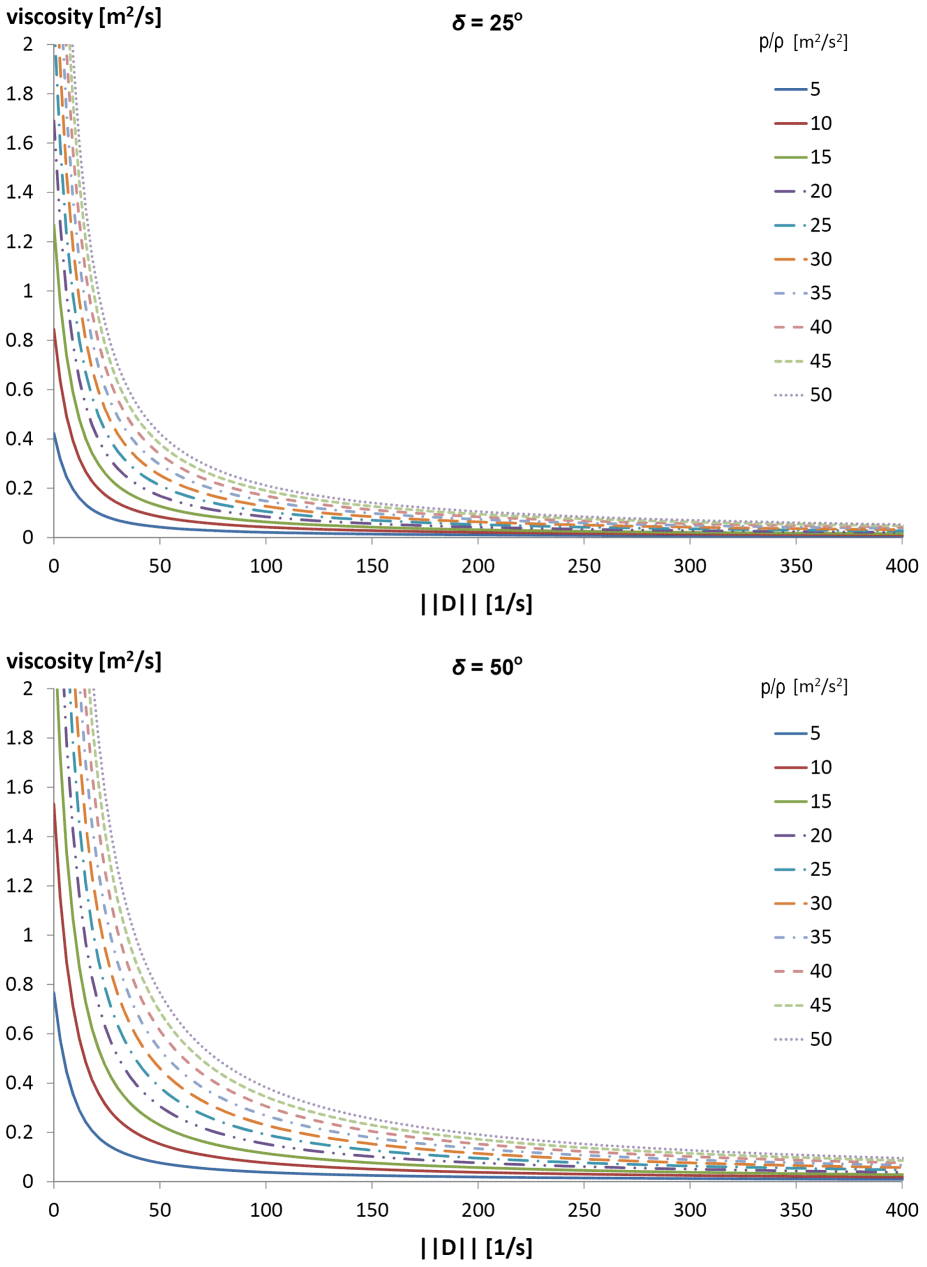

Figure 4. Dependency of the kinematic gravel phase viscosity (for friction angle $\delta = 25^\circ$ and 50°) on the norm of the strain rate tensor $||D||$ at different levels of pressure normalized by density, for $m_y = 0.2$ s

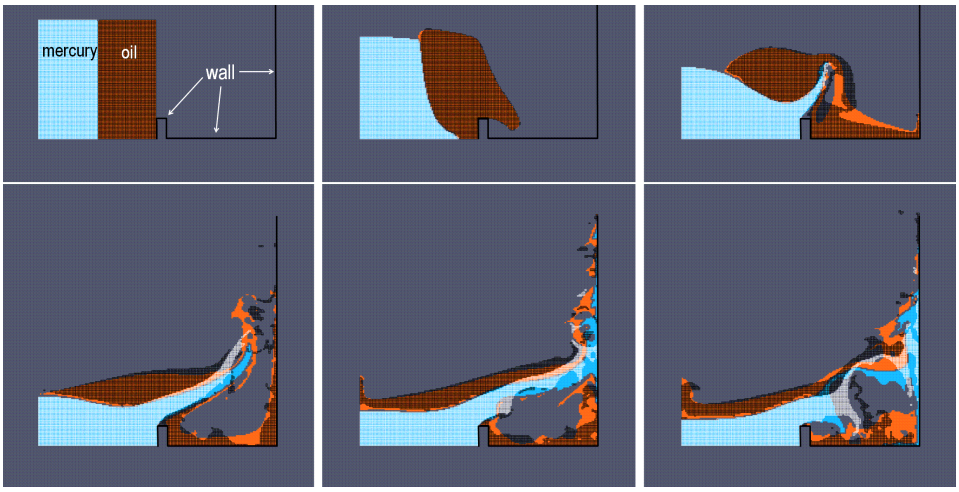

Figure 5. Phase positions in a dam break standard test-case simulation using a drag-based three phase multiphaseEulerFoam simulation (air is transparent, blue indicates mercury and orange represents oil) as background shapes with the corresponding phase positions of our model as wire frame in front (with white mercury as slurry phase and black oil as gravel phase). The visualized time steps correspond to 0, 0.1, 0.2, 0.3, 0.4 and 0.5 seconds.

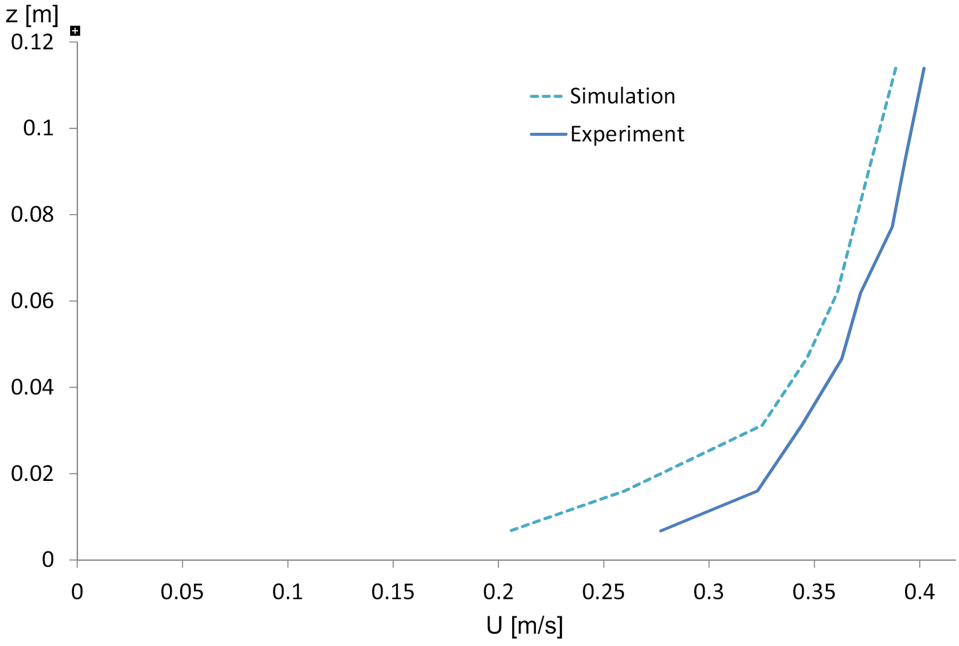

Figure 6. Comparison of simulated and measured average vertical velocity profiles 27 cm away from the channel sidewall of a 1.1 m wide and 40 m long rectangular channel with smooth surface (z is the corresponding height above the bed). In the experiment (Fischer, 1966), a 50.6 l/s inlet discharge was combined with a 0.026% channel inclination resulting in 12.8 cm average flow depth. The simulation applied periodic inlet and outlet boundary conditions and a symmetry plane at the channel center line. Additional calibration of the turbulence model may improve the result.

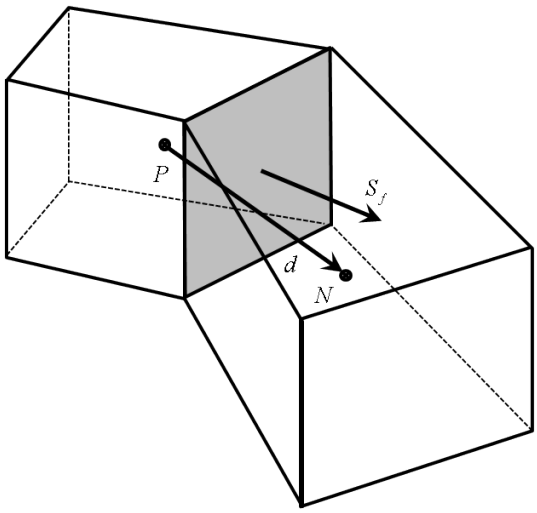

Figure 7. Sketch of two adjacent cells P and N and the shared face f owned by cell P. S_f is the face surface normal vector while d denotes the distance vector from cell center P to cell center N.

Manuscript prepared for Geosci. Model Dev.
with version 2014/09/16 7.15 Copernicus papers of the LaTeX class copernicus.cls.
Date: 31 January 2016

DebrisInterMixing-2.3: A ~~Finite Volume~~ finite volume solver for three dimensional debris flow simulations based on a single calibration parameter. Part one: Model description

A. v. Boetticher[1,3], J. M. Turowski[2,3], B. W. McArdell[3], D. Rickenmann[3], and J. W. Kirchner[1,3]

[1]Department of Environmental Systems Science, ETH Zentrum, CHN H41, 8092 Zürich, Switzerland
[2]Helmholtz-Centre Potsdam GFZ German Research Center for Geosciences, Telegrafenberg, 14473 Potsdam, Germany
[3]Swiss Federal Research Institute WSL, Zürcherstrasse 111, 8903 Birmensdorf, Switzerland

Correspondence to: Albrecht v. Boetticher (albrecht.vonboetticher@usys.ethz.ch)

Abstract. Here we present a three-dimensional fluid dynamic solver that simulates debris flows as a mixture of two ~~phases (gravel and~~ fluids (a Coulomb-Viscoplastic model of the gravel mixed with a Herschel-Bulkley representation of the fine material suspension) ~~with a third~~ in combination with an additional unmixed phase representing the air and the free surface. We link all rheological parameters to the material composition, i. e., to water content, clay content and mineral composition, content of sand and gravel, and the gravel's friction angle; the user must specify only a single free model parameter. The ~~Volume-Of-Fluid~~ Volume-of-Fluid (VOF) approach is used to combine the ~~three phases~~ mixed phase and the air phase into a single cell-averaged Navier-Stokes equation for incompressible flow, based on code adapted from standard solvers of the Open-Source CFD software OpenFOAM. ~~We present a stable implementation of a Coulomb-Viscoplastic model that represents the pressure-dependent flow behavior of the granular phase, and a Herschel-Bulkley representation of the interstitial fluid.~~ The VOF method saves computational costs compared to drag-force based multiphase models. Thus depth-averaging is not necessary and complex three-dimensional flow structures can be simulated while accounting for the pressure- and shear-rate-dependent rheology.

1 Introduction

Debris flows typically occur in steep mountain channels. They are characterized by unsteady flows of water together with different contents of clay, silt, sand, gravel, and larger particles, resulting in a dense and often rapidly moving fluid mass. They are often triggered by heavy rainfall and can

cause massive damage (Petley et al., 2007; Hilker et al., 2009). Their importance has increased due to intense settlement in mountainous regions and also due to their sensitivity to climate change (Guthrie et al., 2010). Their damage potential is not limited to direct impact; severe damage can also be caused by debris flows blocking channels ~~,~~ and thus inducing over-topping of the banks by subsequent flows.

Modeling debris flows is a central part of debris-flow research, because measuring the detailed processes in debris-flow experiments or in the field is challenging. It is still uncertain how laboratory tests can be scaled to represent real flow events, and the inhomogeneous mixture of gravel and fine material brings about interactions of granular flow and viscous forces like drag and pore-pressure that are difficult to track with the present measurement techniques at reasonable cost. As a consequence, the rheological behavior of debris flow material is incompletely understood.

Typically, ~~existing~~ current numerical modeling approaches cannot predict run-out distances or impact pressures of debris flows in known terrain without prior parameter calibration, based on simulating previous well-documented events that happened at the same site. ~~Clearly, this~~ This clearly represents a challenge in practical applications, because ~~often~~ reliable calibration data are ~~unavailable~~rarely available. In addition, the interactions between the granular and ~~viscous~~ fluid phases, and the dynamic change in granular and ~~viscous~~ fluid concentrations during the flow process, limit simple models to the narrow range of simulations that they have been calibrated for, where the fitted parameters account for these interactions. Complex models such as depth-averaged fluid simulations coupled to three dimensional particle methods are associated not only with high computational costs but also with a large number of model parameters, making model calibration the key issue for application to specific cases. This limits the possibilities of using debris flow models as a valid standard application in practice, because the user's ability to estimate values of poorly constrained parameters influences the results.

Here, we present an improved ~~three-phase~~ multiphase modeling approach as an alternative. We provide a coarse but effective solution linking the rheological model of the debris-flow material to field values such as ~~grain-size~~ grain size distribution and water content. The approach aims to link the knowledge of field experts for estimating the release volume and material composition with recent advances that account for complex flow phenomena using three-dimensional computational fluid dynamics. The parameters of the two resulting rheology models for the two mixing ~~phases~~ fluids are linked to material properties such that the model setup can be based on material samples collected from the field, yielding a model that has only one free parameter for calibration.

2 ~~Modeling approach~~

1.1 ~~A two phase model with pressure- and shear-rate-dependent rheology~~

~~Based on a Finite Volume solver for a mixed three-phase incompressible Navier-Stokes equation, we apply two rheology models for two phases that can mix: one for~~ One mixing phase represents the suspension of ~~fine material and water , and one for gravel. We allow interactions of both rheologies, while keeping a third phase unmixed, accounting for the air forming the~~ finer particles with water (also simply called slurry in this paper) and a second mixing phase accounts for the pressure-dependent flow behavior of gravel. A third gas phase is kept unmixed to model the free surface. ~~In this way, the coupling between driving forces, topography and flow-dependent internal friction~~ The focus is on the flow and deposition process and the release body needs to be user-defined. Although, some aspects of material mobilization can be addressed ~~for each phase separately, accounting for the fundamental differences in flow mechanisms of granular and viscous flow (Fig. 1) . Numerical costs are kept reasonable by using the Volume of Fluid method such that only one Navier-Stokes equation system is solved for all three phases. We calculate the viscosityand density of each grid cell as a concentration-weighted average between the viscosities of the phases that are present in the cell. Phase interaction is reduced to this averaging of density and viscosity with the aim to avoid the standard approach of~~ by locally altering the concentration of the slurry phase and the water content of the slurry defined in the material properties, this is not within the scope of this paper.

Table 1. Nomenclature

α	phase fraction
α_m	fraction of the debris mixture (slurry + gravel)
$\boldsymbol{U}$	velocity
$\boldsymbol{Uc}$	inter-facial compression velocity
t	= time
$\mathbf{T}, \mathbf{T_s}$	deviatoric viscous stress tensor (s for granular phase)
$\mathbf{D}$	strain rate tensor
ρ	phase-averaged density, $\rho_i (i = 1, 2, 3)$ density of phase i, ρ_{exp} is a bulk density in experiment
p, p_d	pressure resp. modified pressure
D_{diff}	diffusion constant
ϕ	volumetric flux (ϕ_ρ denotes mass flux, ϕ_r surface-normal flux)
$\mathbf{I}$	identity matrix
μ	phase-averaged dynamic viscosity, $\mu_i (i = 1, 2, 3)$ viscosity of phase phase i
μ_0	maximal dynamic viscosity
μ_{min}	minimal dynamic viscosity
μ_s	Coulomb-viscoplastic dynamic viscosity
∇	gradient
σ	free surface tension coefficient
κ	free surface curvature
$\boldsymbol{g}$	gravitational acceleration
τ	shear stress
τ_y	yield stress of slurry phase (τ_{y-exp} is a measured yield stress)
k	Herschel-Bulkley consistency factor
n	Herschel-Bulkley exponent
$\dot{\gamma}$	shear rate
C	volumetric solid concentration
P_0	volumetric clay concentration
P_1	reduced P_0 in case of high clay content
τ_{00}	free model parameter (affects slurry phase rheology)
τ_0	modified τ_{00} in case of high C
τ_{0s}	yield stress of granular phase modeled with Coulomb friction
β	slope angle
δ	internal friction angle approximated as angle of repose
m_y	constant model parameter (would affect gravel phase rheology)

2 Modeling approach

The debris flow material can be subdivided into a combination of a granular phase mixed with an interstitial fluid composed of the fine material suspension. The latter was successfully modeled in the past as a shear-rate dependent Herschel-Bulkley fluid (Coussot et al., 1998). Because pressure and shear drive the energy dissipation of particle-to-particle contacts, the shear rate substantially influences the energy dissipation within the granular phase. While the two-phase models of Iverson and Denlinger (2001) and Pitman and Le (2005) ~~, we apply linear averaging for simplicity, although non-linear averaging of viscosity between phases may be introduced in the future. The central assumption for concentration-weighted averaging is~~ treated the granular phase as a shear-rate independent Mohr-Coulomb plastic material, dry granular material has been successfully modeled as a viscoplastic fluid by Ancey (2007), Forterre and Pouliquen (2008), Balmforth and Frigaard (2007) and Jop et al. (2006). We follow the suggestions given by Pudasaini (2012) to account for the non-Newtonian behavior of the fluid and the shear- and pressure-dependent Coulomb-viscoplastic behavior of the granular phase, as applied by Domnik et al. (2013). Several modeling approaches to account for the two-phase nature of debris flows used depth-averaged Navier-Stokes equations for each phase coupled by drag models (eg. Bozhinskiy and Nazarov (2000), Pitman and Le (2005), Pudasaini (2012) and Bouchut et al. (2015)). We apply the numerically more efficient method of Iverson and Denlinger (2001) and treat the debris flow material as one mixture with phase-averaged properties described by a single set of Navier-Stokes equations. The resulting reduction in numerical costs allows us to model the three-dimensional momentum transfer in the fluid as well as the free-surface flow over complex terrain and obstacles.

Multiphase flows of gas, fluid and sediment can be addressed with the so-called mixture- or drift-flux model in cases where the local difference in phase velocities is small (Bohorquez, 2008). The properties of all phases are cell-averaged to derive a single mass continuity and momentum balance equation describing the entire mixture. The model presented here has to be seen as a first step, assuming that the local velocity of the gravel is about the same as the velocity of the surrounding fluid, thus allowing us to neglect the drift-flux. This assumption would not be valid for debris flows with little interstitial fluid~~content~~, or with interstitial fluid of small viscosity (i. e., a slurry with low concentrations of fine material). The assumption of equal velocities of both phases in one cell leads to a constant ~~distribution of~~ composition of the mixture by means of phase concentrations over the entire flow process. ~~Nevertheless, this assumption avoids the need to model the drag forces between gravel~~ This basic model can be seen as a counterpart to the mixture model of Iverson and Denlinger (2001), extended by resolving the three dimensional flow structure in combination with a pressure- and ~~interstitial fluid, while still accounting for~~ shear-rate-dependent rheology linked to the material composition. In future work, we aim to relax the constraint of equal phase velocities and allow dispersion of constituents by introducing relative velocities of the gravel phase with respect to the fine sediment suspension according to Bohorquez (2012) and Damián (2013) together with a

coupled Lagrangian particle simulation that can account for larger grains. The basic model presented here focuses on the role of pressure-dependent flow behavior of the gravel, in combination with the shear-dependent rheology of the slurry.

~~Because pressure and shear drive the energy dissipation of particle-to-particle contacts, the shear rate substantially influences the energy dissipation within the granular phase. While the~~ We base our model concept on the well-established finite volume solver interFoam, which is designed for incompressible two-phase ~~models of~~ flow simulations of immiscible fluids ~~and~~ (Deshpande et al., 2012)~~treated the granular phase as a shear-rate independent Mohr-Coulomb plastic material, dry granular material was successfully modeled as a viscoplastic fluid~~. A standard extension named interMixingFoam introduces two mixing phases without momentum exchange coupled to a third unmixed phase by surface tension. Numerical costs are kept reasonable due to the Volume-of-Fluid (VOF) method (Hirt and Nichols, 1981), which solves only one Navier-Stokes equation system for all phases. The viscosity and density of each grid cell is calculated as a concentration-weighted average between the viscosities of the phases that are present in the cell. Between the two mixing phases of gravel and slurry, the interaction reduces to this averaging of density and viscosity. In this way, the coupling between driving forces, topography and three dimensional flow-dependent internal friction can be addressed for each phase separately, accounting for the fundamental differences in flow mechanisms of granular and visco-plastic fluid flow that arise from the presence or absence of Coulomb friction (Fig. 1). We apply linear concentration-weighted averaging of viscosities for estimating the bulk viscosity of a mixture for simplicity. Non-linear averaging of viscosity between phases as suggested by Gao and Li (2012) ~~,~~ may be introduced in the future.

2.1 Governing Equations

Assuming isothermal incompressible phases without mass transfer, we separate the modeled space into a gas region denoting the air and a region of two mixed liquid phases. The VOF method used here determines the volume fractions of all phases in an arbitrary control volume by using an indicator function which yields a phase fraction field for each phase. The phase fraction field represents the probability that a phase is present at a certain point in space and time (Hill, 1998). The air fraction may be defined in relation to the fraction of the mixed fluid α_m as

$$\alpha_1 = 1 - \alpha_m \tag{1}$$

and the mixed fluid α_m may be defined as the sum of the constant fractions of the mixing phases α_2 and α_3:

$$\alpha_m = \alpha_2 + \alpha_3. \tag{2}$$

The flow is defined by the continuity equation together with the transport and momentum equations:

$$\nabla \cdot \boldsymbol{U} = 0, \tag{3}$$

$$\frac{\partial \alpha_m}{\partial t} + \nabla \cdot (\boldsymbol{U} \alpha_m) = 0, \tag{4}$$

and

$$\frac{\partial (\rho \boldsymbol{U})}{\partial t} + \nabla \cdot (\rho \boldsymbol{U} \times \boldsymbol{U}) = -\nabla p + \nabla \cdot \mathbf{T} + \rho \boldsymbol{f}, \tag{5}$$

where $\boldsymbol{U}$ represents the velocity field shared by all phases, $\mathbf{T}$ is the deviatoric viscous stress tensor, ρ is the phase-averaged density, p denotes pressure and $\boldsymbol{f}$ stands for body forces per unit mass like gravity.

An efficient technique of the VOF method is to convect the phase fraction field α_m as an invariant with the divergence-free flow field $\boldsymbol{U}$ that is known from previous time steps:

$$\frac{\partial \alpha_m}{\partial t} + \nabla \cdot (\boldsymbol{U} \alpha_m) + \nabla \cdot (\alpha_1 \boldsymbol{U_c}) = 0, \tag{6}$$

where t denotes time and $\boldsymbol{U_c}$ is an artificial inter-facial compression velocity acting perpendicular to the interface between the gas region and the mixed liquid phases. The method allows a reconstruction of the free surface with high accuracy if the grid resolution is sufficient ~~and~~ (Berberović et al., 2009; Hoang et al., 2012; Deshpande et al., 2012; Hänsch et al., 2013). ~~We follow the suggestions given by~~ The details about the interface compression technique, the related discretization and numerical schemes to solve eq. 6 are given in Deshpande et al. (2012)~~to account for the non-Newtonian behavior of the fluid and the pressure-dependent Coulomb-viscoplastic behavior of the granular phase~~. However, to allow evolving phase concentrations between the mixing phases of the slurry α_2 and the gravel α_3 in future releases, our modified version of the interMixingFoam solver applies eq. 6 separately to each mixing phase including diffusion:

$$\frac{\partial \alpha_i}{\partial t} + \nabla \cdot (\boldsymbol{U} \alpha_i) - D_{diff} \nabla^2 \alpha_i + \nabla \cdot (\alpha_1 \boldsymbol{U_c}) = 0, \tag{7}$$

where $i = 2, 3$ denote the slurry and gravel phases and D_{diff} is the diffusion constant that is set to a negligible small value within the scope of this paper.

The discrete form of eq. 7 is derived by integrating over the volume V of a finite cell of a grid-discretization of the simulated space, which is done in the finite volume method by applying the Gauss Theorem over the cell faces. The advective phase fluxes $\phi_{1..3}$ are obtained by interpolating the cell values of α_1, ~~as applied by~~ α_2 and α_3 to the cell surfaces and by multiplying them with the

flux ϕ through the surface, which is known from the current velocity field. To keep the air phase unmixed, it is necessary to determine the flux ϕ_r through the interface between air and the debris flow mixture, and to subtract it from the calculated phase fluxes $\phi_{1..3}$. Inherited from the original interMixingFoam solver (OpenFOAM-Foundation, 2016a), limiters are applied during this step to bound the fluxes to keep phase concentrations between 0 and 1. With known fluxes $\phi_{1..3}$, the scalar transport equation without diffusion for each phase takes the form

$$\frac{\partial}{\partial t}\alpha_i + \nabla(\phi_i) = 0. \tag{8}$$

Equation 8 is solved using first-order Euler schemes for the time derivative terms, as has been recommended for liquid column breakout simulations (Hänsch et al., 2013).

~~But instead of solving Navier-Stokes equationsfor each phasecoupled by drag models, we apply the numerically more efficient method of and treat the debris flow material as one mixture with~~

After solving the scalar transport equations, the complete mass flux ϕ_ρ from the updated volumetric phase concentrations is constructed:

$$\phi_\rho = \phi_1 \cdot \rho_1 + \phi_2 \cdot \rho_2 + \phi_3 \cdot \rho_3, \tag{9}$$

where $\rho_{1..3}$ denote the constant densities of the corresponding phases and $\phi_{1..3}$ are the corresponding fluxes.

Fig. 2 illustrates how the phase volume distributions α_1 (air), α_2 (slurry) and α_3 (gravel) are used to derive cell-averaged properties of the continuum.

The conservation of mass and momentum is averaged with respect to the phase fraction α of each phase. The density field is defined as

$$\rho = \sum_i \rho_i \alpha_i \tag{10}$$

where ρ_i denotes density of phase i and the density is assumed to be constant.

The deviatoric viscous stress tensor $\mathbf{T}$ is defined based on the mean strain rate tensor $\mathbf{D}$ that denotes the symmetric part of the velocity gradient tensor derived from the phase-averaged ~~properties described by a single Navier-Stokes equation. The resulting reduction in numerical costs allows us to model the three-dimensional momentum transfer in the fluid~~ flow field:

$$\mathbf{D} = \frac{1}{2}[\nabla \boldsymbol{U} + (\nabla \boldsymbol{U})^T], \tag{11}$$

and

$$\mathbf{T} = 2\mu\mathbf{D} - \frac{2}{3}\mu(\nabla\cdot\boldsymbol{U})\mathbf{I}. \tag{12}$$

$\mathbf{I}$ is the identity matrix and μ is the phase-averaged dynamic viscosity, which is simplified in analogy to eq. 10 as the concentration-weighted average of the corresponding phase viscosities:

$$\mu = \sum_i \mu_i \alpha_i \tag{13}$$

The term $\nabla \cdot \mathbf{T}$ in the momentum equation 5 is decomposed as $\nabla \cdot (\mu \nabla \boldsymbol{U}) + \nabla \boldsymbol{U} \cdot \nabla \mu$ to ease discretization. The body forces $\boldsymbol{f}$ in the momentum equation account for gravity and for the effects of surface tension. The surface tension at the interface between the debris flow mixture and air is modeled as a force per unit volume by applying a surface tension coefficient σ. The momentum conservation including gravitational acceleration $\boldsymbol{g}$ and surface tension is defined in our model as:

$$\frac{\partial(\rho\boldsymbol{U})}{\partial t} + \nabla \cdot (\rho\boldsymbol{U} \times \boldsymbol{U}) = -\nabla p_d + \nabla \cdot (\mu \nabla \boldsymbol{U}) + (\nabla \boldsymbol{U}) \cdot \nabla \mu - \boldsymbol{g}\cdot\boldsymbol{x}\nabla\rho + \sigma\kappa\nabla\alpha_1 \tag{14}$$

where κ denotes the local inter-facial curvature and $\boldsymbol{x}$ stands for position. The modified pressure p_d is employed in the solver to overcome some difficulties with boundary conditions in multiphase flow simulations. In case the free surface lies within an inclined wall forming a no-slip boundary condition, the normal component of the pressure gradient must be different for the gas phase and the mixture due to the hydrostatic component ρg. It is common to introduce a modified pressure p_d related to the pressure p by

$$p_d = p - \rho\boldsymbol{g}\cdot\boldsymbol{x}. \tag{15}$$

The gradient of the modified pressure includes the static pressure gradient and contributions that arise from the density gradient as well as ~~the free-surface flowover complex terrain and obstacles.~~ a body force due to gravity (Berberović et al., 2009).

2.1.1 ~~Rheology model for the fine sediment suspension~~

Together with the continuity equation 3 for the multi-phase flow, eq. 14 allows us to calculate the pressure and gravity driven velocities. The corresponding discretization and solution procedure with the PISO (Pressure-Implicit with Splitting of Operators (Issa, 1986)) algorithm is provided in appendix A. In the following section we present the rheology models that define the viscosity components for eq. 13.

2.2 Rheology model for the fine sediment suspension

The viscosity of the gas phase, μ_1 is chosen constant. The introduction of two mixing phases is necessary to distinguish between the pressure-dependent flow behavior of gravel and the shear-thinning viscosity of the suspension of finer particles with water. The rheology of mixtures of water with clay and sand can be described by the Herschel-Bulkley rheology law (Coussot et al., 1998), which defines the shear stress in the fluid as:

$$\tau = \tau_y + k\dot{\gamma}^n \tag{16}$$

where τ_y is a yield stress below which the fluid acts like a solid, k is a consistency factor for the viscosity of the sheared material, $\cancel{\gamma}\ \dot{\gamma}$ is the shear rate and n defines the shear-thinning ($n < 1$) or shear-thickening ($n > 1$) behavior. In OpenFOAM, the shear rate is derived in 3D from the strain rate tensor $\mathbf{D}$:

$$\dot{\gamma} = \sqrt{2 \cdot \mathbf{D} : \mathbf{D}} \tag{17}$$

The shear rate is based on the strain rate tensor to exclude the rotation velocity tensor that does not contribute to the deformation of the fluid body. The model can be rewritten as a generalized Newtonian fluid model to define the shear-rate-dependent effective kinematic viscosity of the slurry phase as:

$$\mu_2 = k|\dot{\gamma}|^{n-1} + \tau_y|\dot{\gamma}|^{-1} \tag{18}$$

if the viscosity is below an upper limit μ_0 and

$$\mu_2 = \mu_0 \tag{19}$$

if the viscosity is higher, to ensure numerical stability.

With $n = 1$ the model simplifies to the Bingham rheology model that ~~was~~ has been widely used to describe debris-flow behavior in the past. It may be reasonable to imagine the rheology parameters to be dependent on the state of the flow. However, even with the implicit assumption that the coefficients are a property of the material and not of the state of the flow, the Herschel-Bulkley rheology law was rarely applied in debris-flow modeling due to the large number of rheology parameters. We avoid this problem by assuming the rheology parameters to be defined by measurable material properties as described below.

2.2.1 Determination of rheology model parameters based on material properties

Results from recent publications allow the reduction of the number of free Herschel-Bulkley parameters to one. If the coarser grain fraction is confined to the gravel phase, the Herschel-Bulkley parameters for the finer material can be linked to material properties as measured using simple standard geotechnical tests. According to Coussot et al. (1998), the exponent n can be assumed constant as $1/3$, and k can be roughly estimated as $\cancel{0.3 \cdot \tau_y}$ $b \cdot \tau_y$, where the constant $b = 0.3\mathrm{s}^{-\mathrm{n}}$ for mixtures with maximum grain-sizes < 0.4 mm (Coussot et al., 1998). An approach for estimating the yield stress τ_y based on water content, clay fraction and composition, and the solid concentration of the entire debris flow material was proposed by Yu et al. (2013) as:

$$\tau_y = \tau_0 C^2 e^{22(C \cdot P_1)} \tag{20}$$

where C is the volumetric solid concentration of the mixture, $P_1 = 0.7P_0$ when $P_0 > 0.27$ and $P_1 = P_0$ if $\cancel{P_0 \text{ is smaller}}$ $P_0 <= 0.27$, and

$$P_0 = C_{kaolinite+chlorite} + 1.3C_{illite} + 1.7C_{montmorillonite} \tag{21}$$

where the subscript of C refers to the volumetric concentration ~~of~~ (relative to the total volume of all solid particles and water) of the corresponding mineral. The discontinuity of P_1 at a modified clay concentration of $P_0 = 0.27$ is a coarse adjustment to a ~~more or less~~ more-or-less sudden change observed in the experimental behavior.

For $C < 0.47$, τ_0 is equal to τ_{00} and otherwise τ_0 can be calculated by

$$\tau_0 = \tau_{00} e^{5(C-0.47)} \tag{22}$$

where τ_{00} is the remaining free parameter which we use to account for the grid size dependency of the shear rate (Yu et al., 2013). We recommend a value of $\cancel{\tau_{00} = 30\mathrm{Pa}}$ $\tau_{00} = 30$ Pa as a starting point for calibration. Yu et al. (2013) compared this method of estimating the yield stress τ_y to experimental results they ~~gained~~ obtained from a set of 514 flume experiments with mixtures of water and clay with fine and coarse sand and less than 5 % gravel. They determined the yield stress by releasing the material mixture from a reservoir into an inclined channel of 0.2 m width and by increasing the inclination slightly until remobilization occurred after the material came to rest. The experimental yield stress τ_{y-exp} was then determined as:

$$\tau_{y-exp} = \rho_{exp} g h sin(\phi\beta), \tag{23}$$

where ~~ρ~~ ρ_{exp} is the density of the applied mixture, g the acceleration due to gravity, h the maximum accumulation thickness of the deposit, and ~~ϕ~~ β the slope inclination. In addition, they compared the calculated yield stress of eq. 20 with experimental yield stresses reported by a number of authors including Coussot et al. (1998) and Ancey and Jorrot (2001). Ancey and Jorrot (2001) used 2 mm and 3 mm glass beads in a kaolinite dispersion as well as fine sand-kaolinite-water mixtures. Up to yield stresses of about 200 Pa the yield stresses estimated by eq. 20 fit the observed ones well. Thus, the yield stresses of sand-clay mixtures with water can be estimated using eq. 20 based on the volumetric concentration of the debris in the water-solids mixture and based on the percentages of different clays in the fraction of fine material. Adjustments to the numbers for calculating P_0 may be necessary to account for the activity of other clays.

The remaining uncertainties concern our assumptions ~~are~~ that n is constant at a value of $1/3$, and that ~~$k = 0.3 \cdot \tau_y$ in~~ k can be defined in such simple dependency to τ_y in the presence of coarser sand. Experiments seem to confirm that n increases in presence of coarser material (Imran et al., 2001), but further research is needed to quantify this effect~~, and~~. Remaitre et al. (2005) found n to vary from 0.27 to 0.36. Schatzmann et al. (803) used $n = 0.33$ to reproduce measured curves obtained with a mixture of 27.5 volumetric percent slurry with 30 % gravel where gravel grain-sizes ranged from 3 to 10 mm, and used $n = 0.5$ to fit the Herschel-Bulkley model to the experiment with 22.5 % slurry and 30 % gravel. Based on the laboratory scale experiments that are presented in v. Boetticher et al. (2015) we have chosen $n = 0.34$ to obtain the best fit for the simulation ~~of~~ presented by large-scale debris-flow experiments.

~~2.2.2 Representation of gravel by a Coulomb-viscoplastic rheology~~

2.3 Representation of gravel by a Coulomb-viscoplastic rheology

~~For a satisfactory prediction of run-out and impact, an adequate simulation of the deposition process is necessary.~~ During acceleration and high-speed flow, the shear-thinning behavior of both the ~~viscid~~ fluid and the granular phase dominate the viscosity in our model. However, pressure-dependent friction becomes important as soon as the material experiences high pressures, accompanied by reduction in shear due to decelerations caused by channel slope reduction. Flows of granular material ~~have been successfully~~ could be modeled as viscoplastic fluids (Ancey, 2007; Forterre and Pouliquen, 2008; Balmforth and Frigaard, 2007; Jop et al., 2006) as cited by Domnik and Pudasaini (2012). Based on Ishii (1975), the granular ~~Cauchy stress tensor T_s~~ stress deviator tensor $\mathbf{T_s}$ can be written as:

$$\mathbf{T_s} = -p - \frac{p}{\rho}\mathbf{I} + 2\nu_s\mathbf{D}\mu_s\mathbf{D}, \tag{24}$$

where ~~$\mathbf{D}$ is the rate-of-deformation tensor,~~ $p\mathbf{I}$ is the ~~normalized~~ pressure times the identity matrix and ~~ν_s~~ μ_s is the corresponding ~~kinematic~~ dynamic viscosity, which was modeled by Domnik and Pudasaini (2012) as:

$$\nu\mu_s = \nu\mu_{min} + \frac{\tau_{0s}}{||\mathbf{D}||}[1 - e^{-m_y||\mathbf{D}||}], \tag{25}$$

where ~~ν_{min}~~ μ_{min} is a minimal ~~kinematic~~ dynamic viscosity, τ_{0s} is a ~~density-normalized~~ yield stress, and $||\mathbf{D}||$ is the norm of the strain-rate tensor defined by the authors as:

$$||\mathbf{D}|| = \sqrt{2tr(\mathbf{D}^2)}. \tag{26}$$

In eq. ~~??~~25, m_y is a model parameter with units of s which we will keep constant~~as reasoned~~, for reasons outlined in the following section. Domnik et al. (2013) suggested replacing the yield stress by a pressure-dependent Coulomb friction, ~~$p \cdot sin(\delta)$~~ $psin(\delta)$ where δ is the internal friction angle:

$$\nu_s\mu_3 = \nu\mu_{min} + \frac{p \cdot sin(\delta)}{||\mathbf{D}||}[1 - e^{-m_y||\mathbf{D}||}] \frac{psin(\delta)}{\rho_3||\mathbf{D}||}[1 - e^{-m_y||\mathbf{D}||}] \tag{27}$$

Here, this Coulomb-viscoplastic rheology model is used to describe the gravel phase~~, by calculating the~~. The pressure- and shear-dependent viscosity is calculated in every cell with the corresponding local pressure p and strain-rate tensor $\mathbf{D}$ derived from the phase-averaged flow field.

2.3.1 Gravel phase properties

The Coulomb-viscoplastic rheology law developed by Domnik et al. (2013) includes two parameters: the friction angle δ, and the parameter m_y influencing the transition between yielded and unyielded regions. For smaller values of m_y, the transition is smoother. In the absence of shear, to achieve a viscosity representing a Coulomb friction equal to $p \cdot sin(\delta)$ where p is the local pressure, m_y needs to be equal to ~~one~~1 s. However, the development of ~~ν_s~~ μ_s under large pressure or strong shear is the same for both $m_y = 1$ s and $m_y = 0.2$ s, but parts of the nearly immobile material that face little pressure (in general, immobile material close to the surface) show a significant reduction in viscosity when $m_y = 0.2$ s (Fig. 3). As a consequence, m_y minimally affects debris flow release and flow at large scales, but material with a ~~low~~ shallow flow depth in a run-out plane close to deposition may develop front fingering (which is dependent on, and sensitive to, the value of m_y) by allowing sudden local solidification. We choose m_y to be constant and equal to 0.2 s for all simulations.

For small friction angles, the modeled viscosity of the gravel phase decreases rapidly with increasing shear. Larger friction angles increase the viscosity and extend the pressure dependency to larger shear rates (Fig. 4). We estimated the friction angle δ based on the maximum angle of repose in tilt-table tests of the gravel. In our laboratory experiments, we determined the friction angle in a simple

adaptation of the method of Deganutti et al. (2011) by tilting a large box with loose material until a second failure of the material body occurred.

In analogy to the Herschel-Bulkley implementation, an upper limit for the viscosity is implemented to maintain numerical stability. Pressure-dependent viscosity in the incompressible Navier-Stokes equations causes numerical instability as soon as the eigenvalues of the symmetric part of the local velocity gradient become larger than ~~$1/(2(\delta\eta/\delta p))$ (where η is the local dynamic viscosity)~~$1/(2(\delta\mu/\delta p))$. Following Renardy (1986), we locally limit the viscosity to ~~fulfill this stability criterion~~keep it below a corresponding local stability limit.

3 ~~Solver description~~Quality characteristics of the model

~~The assumption of negligible velocity differences between the gravel particles and the slurry within a finite-volume cell allows the solution of an averaged Navier-Stokes equation for the three phases air, gravel and fluid. Each phase is treated as a continuum. The phases for the slurry and for the gravel inter-penetrate each other, while the air phase is kept separate. The conservation of mass and momentum is averaged with respect to the phase fraction α of each phase. The phase fraction is the probability that a phase is present at a certain point in space and time . With the phase fractions as a representation of the phase volume distribution, a transport equation for each phase can be solved to obtain the change of phase distribution over the last time step. With the updated phase distribution, the pressure and velocity fields are calculated by solving the phase-averaged Navier-Stokes equations. The Volume-of-fluid (VOF) method is used to reconstruct the free surface with convection schemes from the volume fraction distribution . The method allows a surface reconstruction with high accuracy if the grid resolution is sufficient . Fig. 2 illustrates how the phase volume distributions α_1 (air), α_2 (slurry) and α_3 (gravel) are used to derive cell-averaged properties of the continuum.~~

3.1 Effects of time step size on rheology

Because most debris-flow models are depth-averaged and use shallow-water ~~approximated equations, it could be questioned~~ approximations, one could ask why a three-dimensional approach is necessary. Brodani-Minussi and deFreitas Maciel (2012) compared dam-break experiments of a Herschel-Bulkley fluid and its numerical simulations using the VOF approach with published ~~shallow-water equation based~~ shallow-water-equation-based models. Especially for the first instant after the material release, the application of shallow-water equations seems to introduce errors that are propagated throughout the process, leading to erroneous run-out estimates. ~~In addition to the three-dimensional approach, we introduced an iterative step to determine the shear-dependent viscosity without delay for the model to be able to deal with the challenges of a dam-break release.~~

~~We describe the solver below, beginning with a brief introduction to the PISO (Pressure-Implicit with Splitting of Operators) algorithm for solving the incompressible Navier-Stokes equations for phase-averaged mass and momentum conservation. We then address the numerical solution for each phase flow using advection-diffusion equations with focus on the mixing, and finally we describe some aspects of the dependencies between grid resolution, rheology models and solver stability are described.~~

3.2 ~~Calculation of the velocity field~~

~~The solver is based on an adaption and extension of the interMixingFoam solver, which is one of~~ A similar problem arises when modeling debris-flow impacts on obstacles. Simulating the impact of material with velocity-dependent rheology that is kept constant over the time step although it actually changes with the ~~standard solvers of the open source Finite Volume Code OpenFOAM . The Finite Volume method used here is based on a discretization of the incompressible Navier-Stokes equation to describe the fluid dynamics.~~

~~The incompressible Navier-Stokes momentum equation takes the form:~~

$$\frac{\partial \boldsymbol{u}_i}{\partial t} + \frac{\partial \boldsymbol{u}_i \boldsymbol{u}_j}{\partial \boldsymbol{x}_j} = -\frac{\partial p/\rho}{\partial \boldsymbol{x}_i} + \mu \frac{\partial^2 \boldsymbol{u}_i}{\partial \boldsymbol{x}_j \partial \boldsymbol{x}_j},$$

~~where $\boldsymbol{u}_i$ and $\boldsymbol{u}_j$ $(i,j = 1,2,3)$ are the velocity components in the Cartesian directions $1,2,3$ at a place with coordinates $\boldsymbol{x}_i$ and $\boldsymbol{x}_j$~~ changing flow leads to an accumulating over- or underestimation of energy dissipation. In our model, during release of immobile material that accelerates, the viscosity is overestimated over each time step. As a consequence, the velocity at the end of the time step is underestimated, which again amplifies the overestimation of viscosity in the next time step. Conversely, at an impact, the sudden deceleration causes an underestimation of viscosity over the time step length, leading to an overestimated velocity that again amplifies the underestimation of the viscosity in the next time step. ~~p stands for the local pressure and μ and ρ denote kinematic viscosity and density of the fluid. Integrating eq. 14 over the volume V of a finite cell of a grid-discretization of the simulated space leads to a cell-surface based conservation of momentum for the volume V by applying the Gauss Theorem. Integrals over the volume are thereby replaced by integrals over the cell surface:~~

$$\frac{\partial}{\partial t} \int_V {}_i dV + \oint_{\partial V} {}_{ij} dA_j = -\oint_{\partial V} p/\rho dA_i + \oint_{\partial V} \mu \frac{\partial \boldsymbol{u}_i}{\partial \boldsymbol{x}_j} dA_j.$$

~~The Finite Volume Method replaces the integral over a cell surface by a discrete value, obtaining eq. **??** from eq. **??**. The index k denotes values at cell face k, and field parameters without indices denote the corresponding value in the middle of the cell.~~

$$\frac{\partial}{\partial t}V + \sum_k {}_{i\_j}^{k\,k} A_j^k = -\sum_k \frac{p^k}{\rho} A_i^k + \sum \mu \frac{\partial \boldsymbol{u}_i^k}{\partial \boldsymbol{x}_j} A_j^k$$

Together with the conservation of mass, this leads to an equation system defining the velocities depending on pressure for an incompressible fluid. To reduce the system of equations to the number of unknowns it is necessary to calculate the values at the cell surfaces from interpolation between the values at the cell centers of neighboring cells using interpolation schemes, As a result, flow velocities change with changing time step size. Avalanche codes such as RAMMS (Christen et al., 2007) gives a brief description and summary of implemented schemes. All simulations were carried out using first-order Euler schemes for the time derivative terms, as has been recommended for liquid column breakout simulations . Standard Gaussian finite volume integration with linear interpolation, which is of second order with unbounded numerical behavior, was chosen for the gradient derivative, convection and Laplacian terms. A limited surface-normal gradient scheme was applied that blends corrected and uncorrected treatment of cell orthogonality. An unconventional compressive scheme could be used to sharpen the interface, but here a conventional upwind scheme was used, because more research is necessary on the performance of the compressive scheme deal with this problem by calibrating the model to data from previous events at the same location and similar conditions. But changes in release volume or position can lead to different accelerations and corresponding changes in the automatic time step control can alter the development of rheology over time.

The PISO algorithm uses an optional implicit predictor for the velocity field followed by explicit corrector steps. The predictor uses the pressure field of the old time step to estimate a velocity field for the current time stepwhich is in general not divergence-free. With the idea that a correct velocity field should be divergence-free due to continuity, a Poisson equation for the first corrected pressure field at the current time step is formed by taking the divergence of the equation that defines velocity as a function of pressure. With the corrected pressure, a corrected velocity field can be calculated and the corrector step can be repeated until divergence-free velocities are found. For a detailed description with the corresponding matrix equations, implementation and further literature see .

3.2 Solving the multi-phase flows

By knowing the velocity field from the previous time step , the current timestep starts with calculating the current phase concentrations, accounting for the changes by advection and dispersion.

$$\frac{\partial \alpha_i}{\partial t} + (\times\nabla)\alpha_i - D_{diff}\nabla^2\alpha_i = 0,$$

where D_{diff} is As long as a flow stage is reached where the flow stops accelerating, the diffusion constant. Because diffusion is neglected in our model, equation 7 reduces to the advection equation, which can be solved based on the advective phase fluxes $\phi_{1..3}$ for each phase.

~~The phase fluxes are obtained by interpolating the cell values of α_1, α_2 and α_3 to the cell surfaces and by multiplying them with the flux ϕ through the surface, which is known from the current velocity field. To keep the air phase unmixed, it is necessary to determine the flux ϕ_r through the surfaces between air and the debris flow mixture, and to subtract it from the calculated phase fluxes $\phi_{1..3}$ to achieve an impermeable surface. Inherited from the original interMixingFoam solver , limiters are applied during this stepto bound the fluxes to keep phase concentrations between 0 and 1. With known fluxes $\phi_{1..3}$ for each phase, the scalar transport equation for each phase takes the form~~

$$\frac{\partial}{\partial t}\alpha_i + (\phi_i) = 0$$

~~where $i = 1, 2, 3$ denote the phases air, slurry and gravel.~~

~~It is necessary to limit the fluxes or the phase concentrations such that the sum of volumetric concentrations in each cell adds up to one; otherwise the concept of incompressible flow is violated. However, this limiting constraint can lead to changes of total phase volumes conflicting with the conservation of mass. The standard implementation of the interMixingFOAM solver encounters such difficulties. However, we achieved a good solution in our modified code by first solving equation 8 for the slurry phase, then limiting the updated slurry concentrations to values greater than or equal to zero, then solving equation 8 for the gravel concentrations and limiting the updated gravel concentrations to a range between 0 and (1.0 - slurry concentration).~~

~~Because the influence of the air phase on the debris flow simulation is of small importance, a simple solution is obtained when deriving the final air phase concentration as~~

$$\alpha_1 = 1 - \alpha_2 - \alpha_3.$$

~~In this way, for each phase of the debris flow material , negative phase concentrations or values larger than one can be avoided, while still ensuring that the sum of all three phase concentrations adds up to one. The error is concentrated mainly in the air phase and the gravel phase and the chosen bounding results in a stable solver with sufficient conservation of mass for the debris flow material~~influence on the final front velocity should be negligible. Other debris flow models, which do not iteratively adjust viscosity, cannot accurately simulate impacts. Here, our model constitutes a significant improvement, since in the three-dimensional solver we presented, the viscosity bias was reduced by implementing a corrector step: taking the average between the viscosity at the beginning of the time step and the viscosity that corresponds to the velocity field at the end of the time step, the time step is solved again, leading to a better calculation of the velocity. This step can be repeated, according to user specifications, to correct the viscosity several times. Although this procedure increases numerical calculation time, it clearly reduces the time-step dependency of the simulation. Some dependency

on the time step is still present when modeling the collapse of material columns, but the origin of this problem is different because it occurs also for Newtonian fluids.

~~After solving the transport equations, the complete mass flux ϕ_ρ from the updated volumetric phase concentrations is constructed:~~

3.2 Effect of grid resolution on rheology

$\phi_\rho = \phi_1 \cdot \rho_1 + \phi_2 \cdot \rho_2 + \phi_3 \cdot \rho_3$

~~where $\rho_{1..3}$ denotes the densities of the corresponding phases and $\phi_{1..3}$ the corresponding fluxes.~~

3.3 ~~Effect of grid resolution and time step on rheology~~

Since the shear rate influences both viscosity models, a strong influence of grid resolution on viscosity results, because the shear rate is averaged over the cell size. For flows over rough topography this may be less critical, but for laboratory flume experiments with thin shear bands the results may depend on grid resolution. When simulating laboratory flume experiments where debris-flow material accelerated in a relatively narrow and short channel (Scheidl et al., 2013), a cell height of 1.5 mm, which is of the order of the laboratory rheometer gap, was still not fine enough to reach the limit of grid sensitivity. The free model parameter τ_{00} influences the shear-rate-dependent term of the ~~viscous rheology model ,~~ visco-plastic rheology model and can be used to adjust the simulation to the grid resolution. As long as the gravel phase and grid resolution do not change, it should be possible to model different water and clay contents based on one calibration test. However, as the composition changes, both τ_y and τ_{00} must change commensurately, since ~~the~~ a change in yield stress affects the shear rate. Our procedure for adjusting to different mixtures based on one calibrated test is to perform one iteration step for the yield stress of the new mixture~~:~~; by calculating τ_y based on the original τ_{00} value from the calibration test but with the new material composition, an updated yield stress of the new mixture is determined. Raising or lowering τ_{00} by the same ratio as the change from the original yield stress of the calibration test to the updated yield stress generates the final τ_y as it is applied to the simulation of the new mixture.

The viscosity of the granular phase is averaged over the cell faces to avoid discontinuous viscosity jumps between cells, which may cause instability due to the sensitivity of incompressible solvers to pressure-dependent viscosity. However, thin cells that allow a precise calculation of the shear gradient lead to a preferred direction of the smoothing of the granular phase's viscosity which may introduce physically unrealistic behavior. Cell length (in the flow direction), cell width and cell height should at least be of the same order. Especially when front fingering is of interest, a grid resolution test should be carried out, ensuring that ~~no~~ front instability is not caused by a large aspect ratio of the cell dimensions.

~~Another major problem in many models that simulate the release or impact of material with velocity-dependent rheology is that the viscosity is kept constant over each time step although it actually changes with the changing flow. In our model , during release of immobile material that accelerates, the viscosity is overestimated over each time step. As a consequence, the velocity at the end of the time step is underestimated, which again amplifies the overestimation of viscosity in the next time step. Conversely, at an impact, the sudden deceleration causes an underestimation of viscosity over the time step length, leading to an overestimated velocity that again amplifies the underestimation of the viscosity in the next time step. In both situations, the error sums up from time step to time step. As a result, flow velocities change with changing time step size. Avalanche codes such as RAMMS deal with this problem by calibrating the model to data from previous events at the same location and similar conditions. But changes in release volume or position can lead to different accelerations and corresponding changes in the automatic time step control can change the development of rheology over time. As long as a flow stage is reached where the flow stops accelerating, the influence on the final front velocity should be negligible. Other debris flow models, which do not iteratively adjust viscosity, cannot accurately simulate impacts. Here, our model constitutes a significant improvement, since in the three-dimensional solver presented here, the viscosity bias was reduced by implementing a corrector step: taking the average between the viscosity at the beginning of the time step and the viscosity that corresponds to the velocity field at the end of the time step, the time step is solved again, leading to a better calculation of the velocity. This step can be repeated, according to user specifications, to correct the viscosity several times. Although this procedure increases numerical calculation time, it clearly reduces the time-step dependency of the simulation. Some dependency on the time step is still present when modeling the collapse of material columns, but the origin of this problem is different because it occurs also for Newtonian fluids.~~

4 Discussion

~~Field observations and experiments indicate that the debris flow rheology varies from nearly rigid to highly fluid due to local and temporal variations of pore fluid pressure, shear rate and particle dynamics. In the past, debris flow models have often treated the flowing mixture as a single homogeneous phase with either viscous or granular flowcharacteristics. The traditional approach to the fluid dynamics of debris flows accounted for the vertical momentum exchange in the flow process in a simple manner by assuming a velocity profile over the flow height (concept of depth-averaged shallow-water equations). A good presentation of depth-averaged single phase models, sorted by complexity, is given in . Granular debris flow models addressed the energy dissipation through dispersive shear stress, kinetic stress and collision stress . Dispersive shear stress is caused by the friction between particles in contact as they move past one another during the macroscopic shearing motion. Kinetic~~

~~stress arises when particles at one level in the velocity profile move up or down to another level, and collision stress should account for the sum of energy dissipation due to particle collision . The model of is an example of such a granular perspective linking the energy dissipation in a depth-averaged approach to the basal friction. However, the obvious dependency of the bed friction angle on local topography and velocity led to models with friction angles varying during simulation. One approach was to change the basal friction angle as a function of the Savage number leading to a shear rate and grain size dependent energy dissipation providing a first attempt to link the rheology of the flow to known material properties. In contrast to the approaches outlined above, which addressed debris flows from the granular avalanche perspective, viscoplastic (Coulomb-viscous) theories postulated debris flows as a homogeneous viscoplastic continuum . In viscoplastic approaches, the mechanical behavior of debris flow material is seen as dominated by the influence of a muddy matrix that fills the space between coarser grains. Initially related to Bingham fluids, this matrix behaves like a solid if shear stresses do not exceed a yield stress, and like Newtonian fluids with constant viscosity, if the yield stress is exceeded. If the yield stress is modeled as dependent on the normal stress acting on planes of shearing, one obtains the Coulomb-viscous~~ Because the purpose of this paper is to illustrate the solver structure and model basis, we defer a detailed discussion of model ~~. This model can reproduce the ability of debris flows to move steadily over different slopes. The concept of a yield stress could also explain the observed concentration of deformation in thin bands of sheared layers close to the flow boundaries in channelized debris flows. To account for shear thinning, the Bingham rheology was replaced by a Herschel-Bulkley rheology that can reduce the viscosity at higher shear rates (shear thinning) or increase it (shear thickening), depending on parameter settings. While sand and clay mixtures with water show a shear thinning effect, more granular mixtures exhibit shear thickening~~ performance to the accompanying paper, in which the model is validated against laboratory tests, large scale experiments and natural hill-slope debris flow events. ~~generalized the granular flow model of to account for the presence of pore fluid. With a mixing theory framework, this model was further developed into the Coulomb mixture model, which could simulate a wide spectrum of grain-fluid flows from initiation to deposition, with no redefinition of parameters. It opened the transition from single-phase models to flows composed of solid-fluid mixtures. pointed out that models that treat the debris flow material as a single phase with one rheology are not capable of representing the real behavior, and that a two-phase approach is necessary where one phase accounts for the viscid forces while the second phase models the granular forces between the grains. developed a general two-phase flow model, unifying the single-phase models of , the debris-mixture model of and the two-fluid debris flow model of . Our model can be considered as based on the concept of the Coulomb mixture model but with a state-of-the-art Herschel-Bulkley representation of the fluid and a pressure-dependent Coulomb-viscoplastic representation of the gravel in a three-dimensional approach without depth-averaging~~Here, we discuss only the efficiency of the solver itself, together with a general test about the model accuracy in a gravity-driven open

channel flow. The lack of standard benchmark test cases for debris-flow solvers was the motivation to select a numerical test case to compare model speedup between our approach and a closely related drag-force-based Eulerian multiphase model, and to select a well-defined gravity-driven turbulent open channel flow experiment with clear water to inspect the solver validity.

In comparison to drag-force-based Eulerian multiphase models, the Volume of Fluid approach applied here provides significant reduction in calculation time. For an estimate we compared our model with the OpenFOAM standard solver multiphaseEulerFoam. We selected the official tutorial case damBreak4phaseFine, but turned the water phase into mercury to gain a three-phase test case, and applied the standard solver settings from the case to our model. On a CentOS 6.3 Linux machine with 31 GiB memory and sixteen Intel Xeon CPU E5-2665 @ 2.40 GHz processors, our model resulted in a 5.5 times faster calculation with a comparable collapse of ~~water~~ the modeled mercury and oil columns (Fig. 5). For the sake of completeness our calculation included one iterative viscosity correction step, thus the model efficiency can be estimated to be about ten times higher than a drag-force-based phase coupling approach.

The model was also applied to an open clear water channel experiment with about 50.6 l/s discharge in a 40 m long and 1.1 m wide rectangular smooth channel with 0.026% inclination (Fischer, 1966). The slurry phase was initialized as water together with a zero gravel phase concentration. A Hybrid URANS-LES model was applied to account for the turbulent flow. Instead of an inlet discharge the model applied periodic inlet and outlet boundary conditions and the flow was driven by gravity. The debrisInterMixingFoam solver predicted the discharge of the turbulent channel flow with an underestimation of 15% and underestimated the corresponding surface elevation by 2.5%. However, the deviations in predicted and measured average flow velocities are probably related to shortcomings of the URANS turbulence model at the bottom boundary, as a comparison between a measured and simulated vertical velocity profile suggests (Fig. 6). Due to the lack of a clearly defined benchmark test case for debris flow models, we have chosen this setup as a well-defined larger-scale laboratory test case where the solver faces varying modeled fluid viscosity due to turbulence.

5 Conclusions

The new debris-flow solver has two main strengths. First, it can model three-dimensional flows and their impact against complexly shaped objects, representing the processes at a high level of detail. Second, its design allows simulating different debris flow material compositions without recalibrating the one free parameter, as long as the simulation grid does not change. Due to the solver's pressure- and shear-dependent rheology, realistic deposit geometries and release dynamics can be achieved, as presented and discussed on the basis of test cases in the accompanying paper. By systematically excluding unknown parameters from the model architecture and by accounting for known flow phenomena in a simplified way, we have developed a debris flow model

whose parameters can be ~~estimated directly from site geometry and material compositionrather than from extensive calibration~~ roughly estimated based on material composition, leaving only a single calibration parameter. The concept is promising, ~~but due to high~~ however important parts of phase interactions are neglected in favor of lower numerical costs and ~~long calculation timesthe~~ shorter calculation times. The model is still limited to small simulations of several hundred square meters in surface area unless a powerful computer cluster can be used.

Appendix A: A

The following section describes the detailed implemetation of the PISO iteration procedure as described in Deshpande et al. (2012). By applying the continuum surface force model of Brackbill et al. (1992), the volume integral of eq. 14 is given as

$$\int_{\Omega_i} \frac{\partial \rho \boldsymbol{U}}{\partial t} dV + \int_{\partial\Omega_i} (\rho \boldsymbol{U}\boldsymbol{U}) \cdot \boldsymbol{n} dS = -\int_{\Omega_i} \nabla p_d dV - \int_{\Omega_i} \boldsymbol{g} \cdot \boldsymbol{x} \nabla \rho dV + \int_{\Omega_i} \sigma \kappa \nabla \alpha_1 dV + \int_{\partial\Omega_i} (\mu \nabla \boldsymbol{U}) \cdot \boldsymbol{n} dS + \int_{\Omega_i} \nabla \boldsymbol{U} \cdot \nabla \mu dV. \quad \text{(A1)}$$

The computational domain is discretized into finite-volume cells. Each cell is considered as the owner of exactly one face that it shares with an adjacent neighbor cell, thus each face has a defined owner cell. A surface normal vector S_f with magnitude equal to the surface area of the face is defined on the face pointing outward from the owner cell (Fig. 7). The value at face f of any variable χ calculated in the cell centers as χ_P and χ_N (Fig. 7) can be derived by interpolation using a mixture of central and upwind schemes:

$$\chi_{\mathbf{f}} = \gamma(\chi_P - \chi_N) + \chi_N, \quad \text{(A2)}$$

with a weighting factor γ that can account for the flow direction based on the chosen interpolation scheme and flux limiter. In case of a linear interpolation scheme and a flux limiter ψ, γ can be defined as

$$\gamma = \psi \frac{fN}{d} + (1 - \psi) \frac{\phi_f}{|\phi_f|}, \quad \text{(A3)}$$

where d is the distance between the cell centers P and N and fN is the distance from the face center to the cell center N. The face flux denoted as ϕ_f serves as a switch to account for the flow direction since it turns negative when the flow is from N to P (Berberović et al., 2009). Several limiters are

implemented (OpenFOAM-Foundation, 2016b); we chose the vanLeer scheme and assumed uniform grid spacing to simplify the following explanations with $fN/d = 0.5$.

Variables that are evaluated at the cell faces are subscripted by f. Due to stability problems that arise from the pressure-velocity coupling in collocated meshes (Ferziger and Peric, 2002), the pressure is solved for the cell centers whereas the velocity is interpolated to the cell faces within the PISO loop.

With the switch function

$$\zeta(\phi_f) = \frac{\phi_f}{|\phi_f|} \tag{A4}$$

the velocity $\boldsymbol{U}_f$ at face f can be written based on eq. A2 and A3 as

$$\boldsymbol{U}_f = \frac{\boldsymbol{U}_P}{2}(1+\zeta(\phi_f)(1-\psi)) + \frac{\boldsymbol{U}_N}{2}(1-\zeta(\phi_f)(1-\psi)), \tag{A5}$$

and the corresponding face-perpendicular velocity gradient is given by Deshpande et al. (2012) as

$$\nabla^{\perp}_f \boldsymbol{U} = \frac{\boldsymbol{U_N} - \boldsymbol{U_P}}{|d|}. \tag{A6}$$

At the present time step t^n the phase averaged density of the next time step ρ^{n+1} is known from solving the transport equations. In a first approximation, the corresponding viscosity field μ^{n+1} can be derived accordingly. A simplified formulation of the momentum equation A1 without pressure, surface tension and gravity terms discretized for cell P could then be formulated as

$$\frac{(\rho^{n+1}\tilde{\boldsymbol{U}}) - (\rho^n \boldsymbol{U^n})}{\Delta t}|\Omega_P| + \sum_{f\in\partial\Omega_i} \rho^n{}_f \phi^n{}_f \tilde{\boldsymbol{U}}_f = \sum_{f\in\partial\Omega_i} \mu^{n+1}{}_f \nabla^{\perp}_f \tilde{\boldsymbol{U}} |\boldsymbol{S}_f| + \nabla \boldsymbol{U}^n \cdot \nabla \mu^{n+1} |\Omega_P|. \tag{A7}$$

The tilde stands for the velocity at cell P predicted in the current iterative step, for which eq. A7 yields an explicit expression. For that purpose, eq. A5 and A6 are inserted into eq. A7 using the velocity of the prior iteration step, $\boldsymbol{U^m}$, in all neighbor cells (Deshpande et al., 2012). The explicit expression for the estimated velocity is

$$A_P \tilde{\boldsymbol{U}} = H(\boldsymbol{U^m}), \tag{A8}$$

and by including surface tension and gravity this leads to

$$\tilde{\boldsymbol{U}} = \frac{H(\boldsymbol{U^m})}{A_P} + \frac{\sigma\kappa\nabla\alpha_1^{n+1}}{A_P} - \frac{\boldsymbol{g}\cdot\boldsymbol{x}\nabla\rho}{A_P}. \tag{A9}$$

The detailed composition of $H(\boldsymbol{U^m})$ and A_P formulated with respect to the splitting between neighbor and owner cells can be found in Deshpande et al. (2012); here it is sufficient to keep in mind that $H(\boldsymbol{U^m})$ contains all off-diagonal contributions of the linear system.

The next step is to assemble the approximated face flux

$$\tilde{\phi_f} = \left(\frac{H(\boldsymbol{U^m})}{A_P}\right)_f \cdot \boldsymbol{S}_f + \left(\frac{(\sigma\kappa)^{n+1}(\nabla^\perp{}_f\alpha_1)^{n+1}}{A_P}\right)_f |\boldsymbol{S}_f| - \left(\frac{(\boldsymbol{g}\cdot\boldsymbol{x})^{n+1}(\nabla^\perp{}_f\rho)^{n+1}}{A_P}\right)_f |\boldsymbol{S}_f| \quad \text{(A10)}$$

where the subscript f indicates that the variable values at the faces are used. The final flux is found by adding the pressure contribution

$$\phi^{m+1}{}_f = \tilde{\phi_f} - \left(\frac{\nabla^\perp{}_f p_d^{m+1}}{A_P}\right)_f |\boldsymbol{S}_f|. \quad \text{(A11)}$$

The sum of the flux over the cell faces needs to be zero due to mass conservation for the incompressible flow

$$\sum_{f\in\partial\Omega_i} \phi^{m+1}{}_f = 0, \quad \text{(A12)}$$

Thus the pressure is defined by the linear equation system for the updated pressure ${p_d}^{m+1}$

$$\sum_{f\in\partial\Omega_i} \left(\frac{\nabla^\perp{}_f p_d^{m+1}}{A_P}\right)_f |\boldsymbol{S}_f| = \sum_{f\in\partial\Omega_i} \tilde{\phi_f}, \quad \text{(A13)}$$

and can be solved with the preconditioned conjugate gradient (PCG) algorithm, to mention one of several options implemented in OpenFOAM. With the updated pressure ${p_d}^{m+1}$, the face fluxes $\phi^{m+1}{}_f$ are derived from eq. A11 and the updated velocity filed $\boldsymbol{U}^{m+1}$ is obtained from the explicit velocity correction

$$\boldsymbol{U}^{m+1} = \tilde{\boldsymbol{U}} + \left(\frac{1}{A_P}\right)\left(\sum_{f\in\partial\Omega_i} \frac{(\boldsymbol{S}_f \otimes \boldsymbol{S}_f)}{|\boldsymbol{S}_f|}\right)^{-1} \bullet \left(\sum_{f\in\partial\Omega_i} \left(\frac{\phi^{m+1}{}_f - \tilde{\boldsymbol{U}}_f \cdot \boldsymbol{S}_f}{(\frac{1}{A_P})_f}\right) \frac{\boldsymbol{S}_f}{|\boldsymbol{S}_f|}\right) \quad \text{(A14)}$$

which is the end of the PISO loop. After updating the index m to $m+1$, the iteration restarts with recalculating H with the updated velocity from equation A8, repeating the loop until a divergence-free velocity field is found.

A1 Code availability

The source-code can be downloaded from the supplement application.zip~~, please~~. Please follow the instructions given in the ~~README15~~README.pdf file for installation.

Acknowledgements. We thank Shiva Pudasaini, Johannes ~~Hbl~~ Hübl and Eugenio Oñate for thoughtful critiques and suggestions.

References

Ancey, C.: Plasticity and geophysical flows: a review., J. Non-Newton. Fluid Mech., 142, 4–35, 2007.

Ancey, C. and Jorrot, H.: Yield stress for particle suspensions within a clay dispersion., J. Rheol., 45, 297–319, 2001.

Balmforth, N. and Frigaard, I.: Viscoplastic fluids: from theory to application, J. Non-Newton. Fluid Mech., 142, 1–3, 2007.

Berberović, E., van Hinsberg, N. P., Jakirlić, S., Roisman, I. V., and Tropea, C.: Drop impact onto a liquid layer of finite thickness: Dynamics of the cavity evolution, Phys. Rev. E, 79, 036 306, doi:10.1103/PhysRevE.79.036306, 2009.

Bohorquez, P.: Study and Numerical Simulation of Sediment Transport in Free-Surface Flow, Ph.D. thesis, Universit"at Malaga, Spain, 2008.

Bohorquez, P.: Finite Volume Method of Falling Liquid Films Carrying Monodispersed Spheres in Newtonian Regime, AIChE J, 58, 2601–2616, 2012.

Bouchut, F., Fernandez-Nieto, E. D., Mangeney, A., and Narbona-Reina, G.: A two-phase shallow debris flow model with energy balance, ESAIM-MATHEMATICAL MODELLING AND NUMERICAL ANALYSIS-MODELISATION MATHEMATIQUE ET ANALYSE NUMERIQUE, 49, 101–140, 2015.

Bozhinskiy, A. N. and Nazarov, A. N.: Two-phase model of debris flow, in: 2nd International Conference on Debris-Flow Hazards Mitigation, pp. 16–18, Teipei, Taiwan, 2000.

Brackbill, J. U., Kothe, D. B., and Zemach, C.: A continuum method for modeling surface tension, J. Comput. Phys., 100, 335–354, 1992.

Brodani-Minussi, R. and deFreitas Maciel, G.: Numerical Experimental Comparison of Dam Break Flows with non-Newtonian Fluids, J. of the Braz. Soc. of Mech. Sci. and Eng., 34-2, 167–178, 2012.

Christen, M., Bartelt, P., and Gruber, U.: RAMMS - a Modelling System for Snow Avalanches, Debris Flows and Rockfalls based on IDL, Photogramm. Fernerkund. Geoinf., 4, 289–292, 2007.

Coussot, P., Laigle, D., Aratano, M., Deganuttil, A., and Marchi, L.: Direct determination of rheological characteristics of debris flow, J Hydraul Eng, pp. 865–868, 1998.

Damián, S. M.: An extended mixture model for the simultaneous treatment of schort and long scale interfaces, Ph.D. thesis, Universidad Nacional de Litoral, Argentina, 2013.

Deganutti, A., Tecca, P., and Genevois, R.: Characterization of friction angles for stability and deposition of granular material, in: Italian Journal of Engineering and Environment: 5th International Conference on Debris-Flow Hazards: Mitigation, Mechanics, Prediction and Assessment, pp. 313–318, Padua, Italy, 2011.

Deshpande, S. S., Anumolu, L., and Trujillo, M. F.: Evaluating the perfomance of the two-phase flow solver interFoam, Computational Science and Discovery, 5, 1–33, 2012.

Domnik, B. and Pudasaini, S.: Full two-dimensional rapid chute flows of simple viscoplastic granular materials with a pressure-dependent dynamic slip-velocity and their numerical simulations, J. Non-Newton. Fluid Mech, 173–174, 72–86, 2012.

Domnik, B., Pudasaini, S., Katzenbach, R., and Miller, S.: Coupling of full two-dimensional and depth-averaged models for granular flows, J. Non-Newton. Fluid Mech, 201, 56–68, 2013.

Ferziger, J. H. and Peric, M.: Computational Methods for Fluid Dynamics, Springer 3rd ed., Berlin, 2002.

Fischer, H. B.: Longitudinal Dispersion in Laboratory and Natural Streams, Ph.D. thesis, California Institute of Technology, 1966.

Forterre, Y. and Pouliquen, O.: Flows of dense granular media, Annu. Rev. Fluid Mech., 40, 1–24, 2008.

Gao, Y. and Li, K.: New models for calculating the viscosity of mixed oil, Fuel, 95, 431–437, 2012.

Guthrie, R., Mitchell, J., Lanquaye-Opoku, N., and Evans, S.: Extreme weather and landslide initiation in coastal British Columbia, Journal of engineering geology and hydrogeology, 43, 417–428, 2010.

Hänsch, S., Lucas, D., Höhne, T., Krepper, E., and Montoya, G.: Comparative simulations of free surface flows using VOF-methods and a new approach for multi-scale interfacial structures, in: Proceedings of the ASME 2013 Fluids Engineering Summer Meeting, Incline Village, Nevada, USA, 2013.

Hilker, N., Badoux, A., and Hegg, C.: The Swiss flood and landslide damage database 1972-2007, Nat. Hazards Earth Syst. Sci., 9, 913–925, 2009.

Hill, D.: The Computer Simulation of Dispersed Two-Phase Flows, Ph.D. thesis, Imperial College, University of London, 1998.

Hirt, B. and Nichols, B.: Volume of Fluid (VOF) Method for the Dynamics of Free Boundaries, Journal of Computational Physics, 39, 201–225, 1981.

Hoang, D., van Steijn, V., Kreutzer, M., and Kleijn, C.: Modeling of Low-Capillary Number Segmented Flows in Microchannels Using OpenFOAM, in: Numerical Analysis and Applied Mathematics ICNAAM 2012, AIP Conf. Proc., vol. 1479, pp. 86–89, Kos Island, Greece, 2012.

Hürlimann, M., McArdell, W., and Rickli, C.: Field and laboratory analysis of the runout characteristics of hillslope debris flows in Switzerland, Geomorphology, 232, 20–32, doi:10.1016/j.geomorph.2014.11.030, 2015.

Imran, J., Parker, G., Locat, J., and Lee, H.: 1D numerical model of muddy subaqueous and subaerial debris flows, J Hydraul. Eng., pp. 959–968, 2001.

Ishii, M.: Thermo-Fluid Dynamic Theory of Two-Phase Flow, Eyrolles, Paris, 1975.

Issa, R.: Solution of the implicitly discretized fluid-flow equations by operator-splitting, J Comp. Phys., 62, 40–65, 1986.

Iverson, R. and Denlinger, P.: Flow of variably fluidized granular masses across three-dimensional terrain: 1. Coulomb mixture theory, J. Geophys. Res., 106, 537–552, 2001.

Jop, P., Forterre, Y., and Pouliquen, O.: A constitutive law for dense granular flows, Nature, 441, 727–730, 2006.

OpenFOAM-Foundation: OpenFOAM Standard Solvers, Website User Guide of OpenFOAM, http://www.openfoam.org/docs/user/standard-solvers.php, visited 12.01.2016., 2016a.

OpenFOAM-Foundation: OpenFOAM Standard Schemes, Website User Guide of OpenFOAM, http://cfd.direct/openfoam/user-guide/fvSchemes/, visited 12.01.2016., 2016b.

Petley, D. N., Hearn, G. J., Hart, A., Rosser, N. J., Dunning, S. A., Oven, K., and Mitchell, W. A.: Trends in landslide occurence in Nepal, Nat Hazards, 43, 23–44, 2007.

Pitman, E. and Le, L.: A two-fluid model for avalanche and debris flows, Philos. Trans. R. Soc. A, 363, 1573–1602, 2005.

Pudasaini, S.: A general two-phase debris flow model, J. Geophys. Res., 117, F03 010, 2012.

Remaitre, A., Malet, J., Maquaire, O., Ancey, C., and Locat, J.: Flow behaviour and runout modelling of a complex derbis flow in a clay-shale basin, Earth Surf Proc Landforms, 30, 479–488, 2005.

Renardy, M.: Some remarks on the Navier-Stokes Equations with a pressure-dependent viscosity, Comm. in Partial Differential Equations, 11, 779–793, 1986.

Schatzmann, M., Fischer, P., and Bezzola, G. R.: Rheological Behavior of Fine and Large Particle Suspensions, J. Hydraul Eng.-ASCE, 796, 391–430, 803.

Scheidl, C., Chiari, M., Kaitna, R., Müllegger, M., Krawtschuk, A., Zimmermann, T., and Proske, D.: Analysing Debris-Flow Impact Models, Based on a Small Scale Modelling Approach, Surv. Geophys, 34, 121–140, 2013.

v. Boetticher, A., Turowski, J. M., McArdell, W. B., Rickenmann, D., Hürlimann, M., Scheidl, C., and Kirchner, J. W.: (submitted) DebrisInterMixing-2.3: A Finite Volume solver for three dimensional debris flow simulations based on a single calibration parameter. Part two: Model validation, Geoscientific Model Development, 2015.

Yu, B., Ma, Y., and Qi, X.: Experimental Study on the Influence of Clay Minerals on the Yield Stress of Debris Flows, J. Hydraul. Eng., 139, 364–373, 2013.

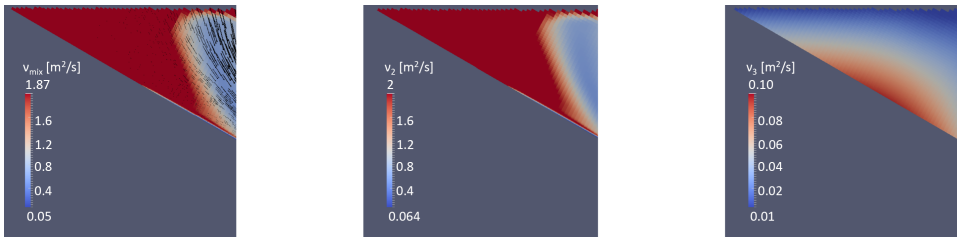

Figure 1. Viscosity distribution (indicated by color scale) along a 28 cm long section through the modeled 0.01 m^3 release block 0.2 s after release, corresponding to the experimental setup of Hürlimann et al. (2015). The starting motion (black velocity arrows) with corresponding viscosity distribution of the mixture (left) is a consequence of blending pure shear-rate dependent ~~mud phase~~ slurry-phase rheology (center) with the pressure- and shear-rate-dependent gravel phase rheology that accounts for Coulomb friction (right). Because the gravel concentration in this example is low, its effect on the overall viscosity is small.

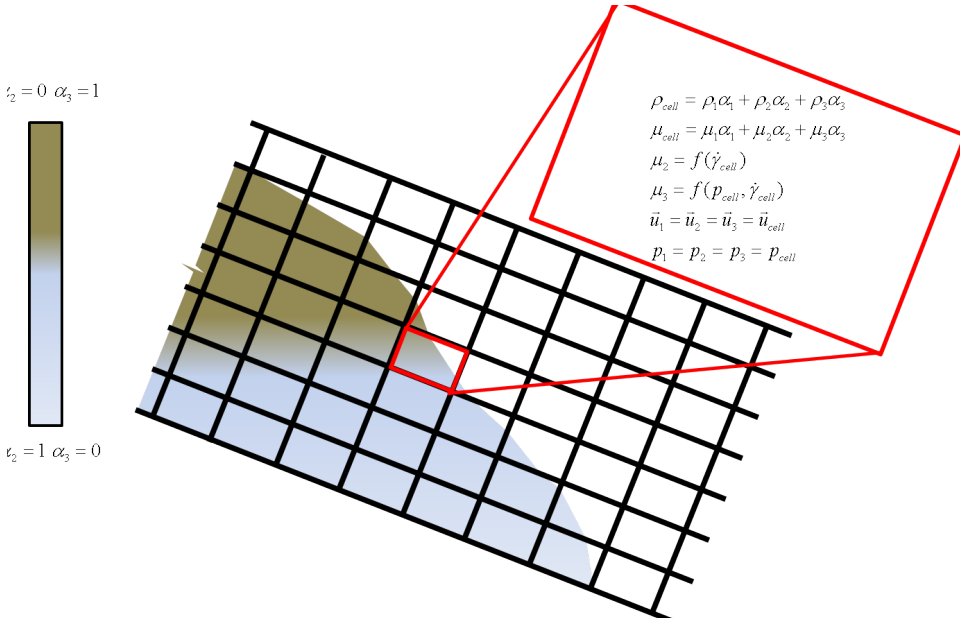

Figure 2. Longitudinal section through a debris flow front discretized with finite volume-cells, showing the constitutive equations for one cell with density ρ and viscosity μ given the densities $\rho_{1..3}$, viscosities $\mu_{1..3}$ and proportions $\alpha_{1..3}$ of phases present. 1 denotes air (white colored cell content), 2 the mud and 3 the gravel phase, respectively.

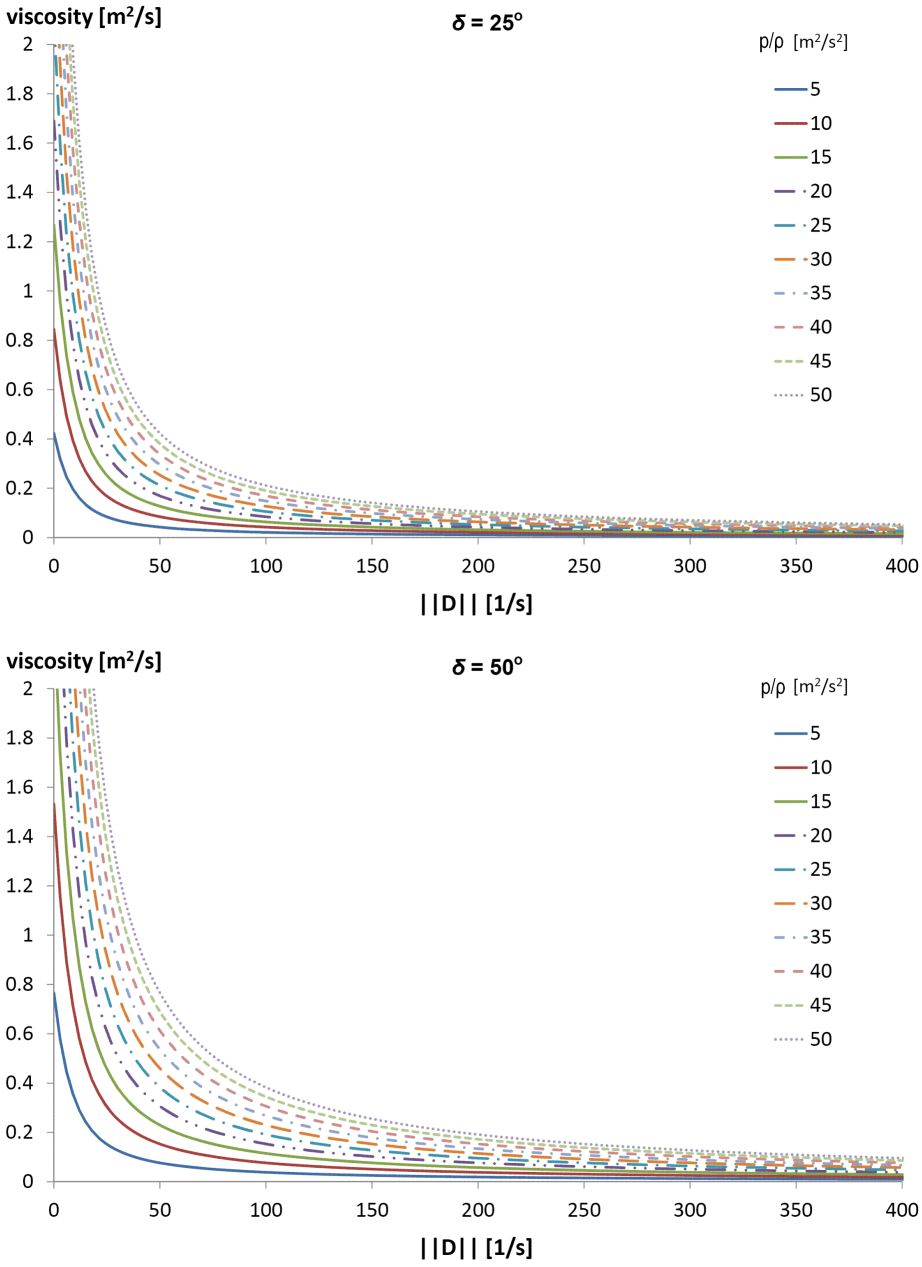

Figure 4. Dependency of the kinematic gravel phase viscosity (for friction angle $\delta = 25^\circ$ and 50°) on the norm of the strain rate tensor $||D||$ at different levels of pressure normalized by density, for ~~$m = 0.2$~~$m_y = 0.2$ s

~~Longitudinal section through a debris flow front discretized with finite volume cells, showing the constitutive equations for one cell with density ρ and viscosity μ given the densities $\rho_{1..3}$, viscosities $\mu_{1..3}$ and proportions $\alpha_{1..3}$ of phases present. 1 denotes air (white colored cell content), 2 the mud and 3 the gravel phase,~~

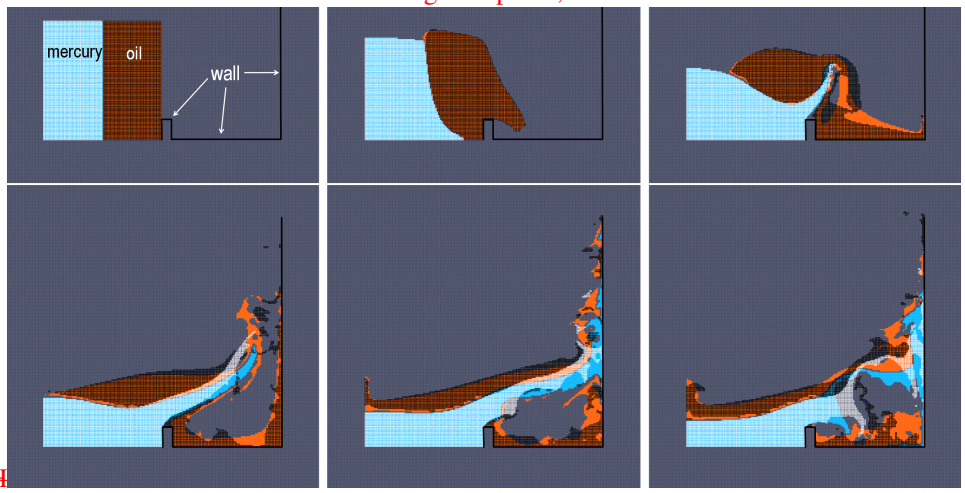

~~respectively.H~~

Figure 5. Phase positions in a dam break standard test-case simulation using a drag-based three phase multiphaseEulerFoam simulation (air is transparent, blue indicates mercury and orange represents oil) as background shapes with the corresponding phase positions of our model as wire frame in front (with white mercury as slurry phase and black oil as gravel phase). The visualized time steps correspond to 0, 0.1, 0.2, 0.3, 0.4 and 0.5 seconds.

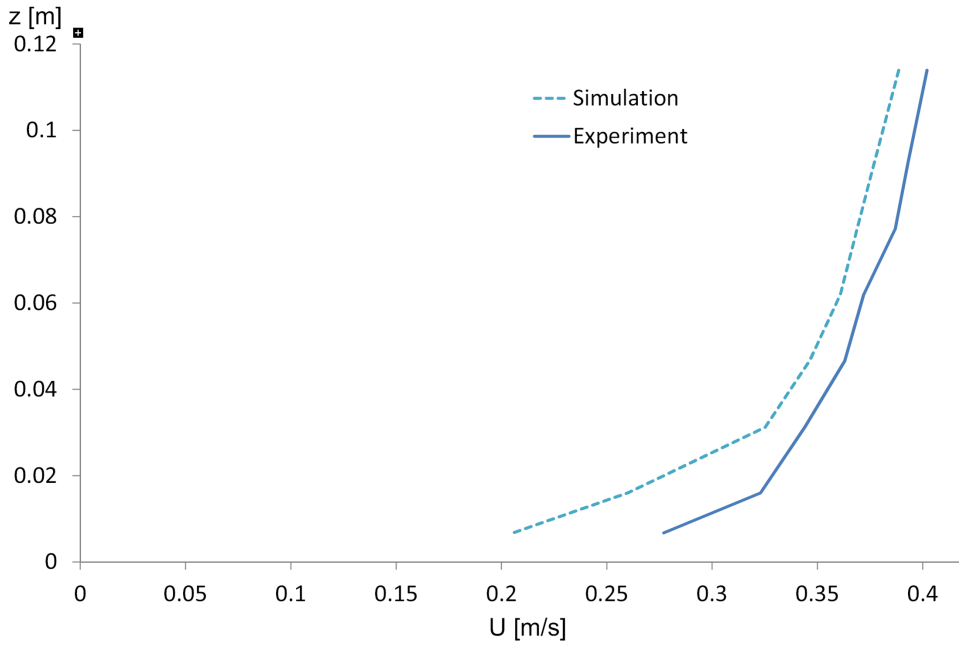

Figure 6. Comparison of simulated and measured average vertical velocity profiles 27 cm away from the channel sidewall of a 1.1 m wide and 40 m long rectangular channel with smooth surface (z is the corresponding height above the bed). In the experiment (Fischer, 1966), a 50.6 l/s inlet discharge was combined with a 0.026% channel inclination resulting in 12.8 cm average flow depth. The simulation applied periodic inlet and outlet boundary conditions and a symmetry plane at the channel center line. Additional calibration of the turbulence model may improve the result.

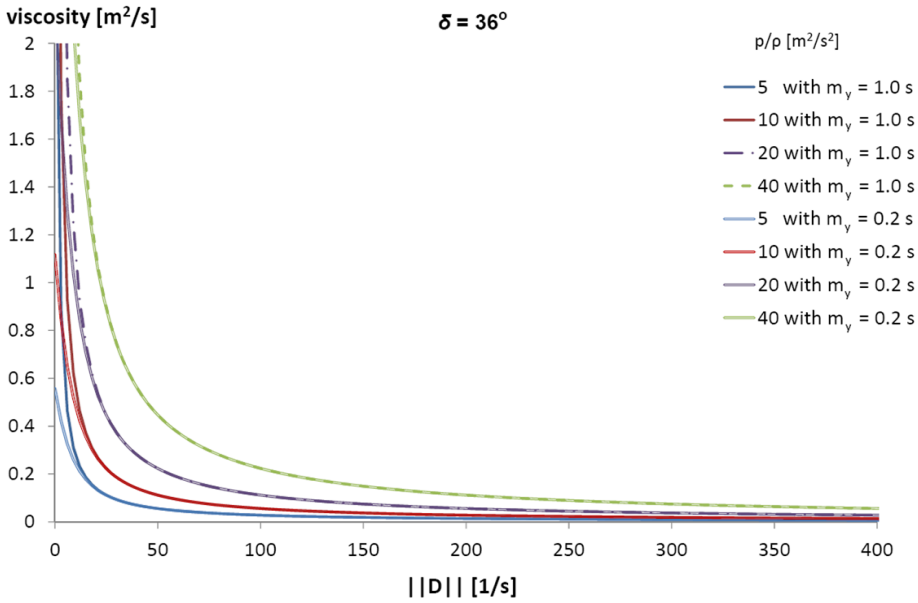

Figure 3. Dependency of the kinematic gravel phase viscosity ν_s (~~for friction angle $\delta = 36°$~~normalized by density) on the norm of the strain rate tensor $||D||$ at different levels of pressure normalized by density, for ~~$m = 1$~~$m_y = 1$ s and ~~$m = 0.2$~~$m_y = 0.2$ s and a friction angle $\delta = 36°$.

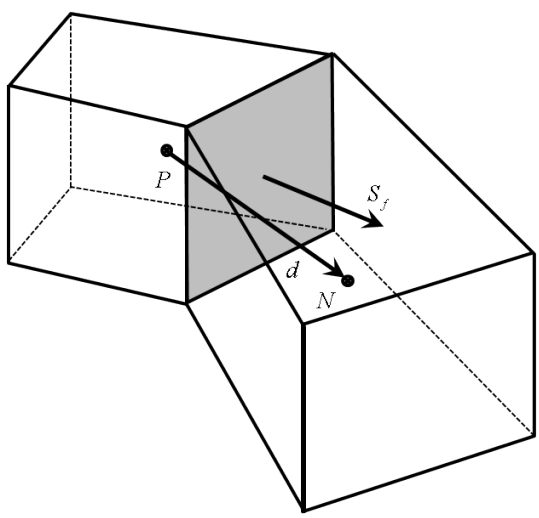

Figure 7. Sketch of two adjacent cells P and N and the shared face f owned by cell P. S_f is the face surface normal vector while d denotes the distance vector from cell center P to cell center N.